ELONGATED HYPOCOTYL 5 mediates blue light signalling to the *Arabidopsis* circadian clock.

Anita Hajdu[1,6], Orsolya Dobos[1,6], Mirela Domijan[2], Balázs Bálint[3], István Nagy[3], Ferenc Nagy[1,4], László Kozma-Bognár[1,5,*]

[1]Institute of Plant Biology, Biological Research Centre, Szeged, H-6726, Hungary
[2]Department of Mathematical Sciences, University of Liverpool, Liverpool, L69 7ZL, United Kingdom
[3]SeqOmics Ltd, Mórahalom, H-6782, Hungary
[4]Institute of Molecular Plant Sciences, University of Edinburgh, Edinburgh, EH9 3BF, United Kingdom
[5]Department of Genetics, Faculty of Sciences and Informatics, University of Szeged, Szeged, H-6726, Hungary
[6]These authors contributed equally to this work.

*To whom correspondence should be addressed:
László Kozma-Bognár
phone: +36-62-599-717
fax: +36-62-433-434
e-mail: kozma_bognar.laszlo@brc.mta.hu

Running head: HY5 relays light signals to the circadian clock

Keywords: circadian clock, light entrainment, blue light, chromatin association, gene expression, HY5 transcription factor, photoreceptors, *Arabidopsis thaliana*

Total word count: 7603; summary: 197; introduction: 1049; results: 2580; discussion: 973; experimental procedures: 1402; figure legends: 1350; acknowledgements: 52; references: 2061.

SUMMARY

Circadian clocks are gene networks producing 24-h oscillations at the level of clock gene expression that is synchronized to environmental cycles via light signals. The ELONGATED HYPOCOTYL 5 (HY5) transcription factor is a signalling hub acting downstream of several photoreceptors and is a key mediator of photomorphogenesis. Here we describe a mechanism by which light quality could modulate the pace of the circadian clock through governing abundance of HY5.

We show that *hy5* mutants display remarkably shorter period rhythms in blue but not in red light or darkness and blue light is more efficient than red to induce accumulation of HY5 at transcriptional and post-transcriptional levels. We demonstrate that the pattern and level of HY5 accumulation modulates its binding to specific promoter elements of majority of clock genes, but only a few of these show altered transcription in the *hy5* mutant. Mathematical modelling suggests that the direct effect of HY5 on the apparently non-responsive clock genes could be masked by feed-back from the clock gene network. We conclude that the information on the ratio of blue and red components of the white light spectrum is decoded and relayed to the circadian oscillator, at least partially, by HY5.

SIGNIFICANCE STATEMENT

Resetting the circadian clock by light involves modulation of clock gene transcription, but the molecular details of this process are poorly understood. We show that transcription factor HY5, a key component of general light signalling cascades, binds to and affects transcription of several core clock genes. We demonstrate that blue light is more effective than red light to increase HY5 protein levels, revealing a potential mechanism by which light quality could influence the clock.

INTRODUCTION

Daily rhythms in physiology are common to all organisms that are exposed to the succession of days and nights. Most of these rhythms are driven by endogenous timekeepers, called circadian clocks, so that they can persist even under constant conditions. However, the most important biological function of circadian clocks and overt rhythms is to schedule molecular and cellular processes to the most appropriate time of the day. Having these processes shut down at times when they are not needed saves considerable amounts of energy and resources that confers competitive advantage to organisms possessing clocks resonating with environmental cycles (Ouyang *et al.*, 1998, Dodd *et al.*, 2005).

Eukaryotic circadian oscillators are built on transcriptional/translational negative feedback loops that are operated by mutual interactions among the so-called clock genes and the corresponding clock proteins. The structure of the plant clock is highly complicated and relies on four interconnected regulatory loops (Foo *et al.*, 2016). Recent reviews provide detailed descriptions of the oscillator (Hsu and Harmer, 2014, Greenham and McClung, 2015). *CIRCADIAN CLOCK ASSOCIATED 1* (*CCA1*) and *LATE ELONGATED HYPOCOTYL* (*LHY*) encode Myb-related transcription factors that are expressed in the morning (Schaffer *et al.*, 1998, Wang and Tobin, 1998), but are repressed throughout the day until midnight by the sequentially expressed PSEUDO-RESPONSE REGULATOR (PRR) 9, 7, 5 and PRR1/TOC1 proteins (Nakamichi *et al.*, 2010, Huang *et al.*, 2012). CCA1 and LHY act as general repressors within the clock circuit (Adams *et al.*, 2015, Kamioka *et al.*, 2016) inhibiting the expression of *LUX ARRHYTHMO* (*LUX*), *EARLY FLOWERING 3* (*ELF3*) and *EARLY FLOWERING 4* (*ELF4*), among others (Helfer *et al.*, 2011, Herrero *et al.*, 2012, Lu *et al.*, 2012). LUX, ELF3 and ELF4 form the core of the so-called Evening Complex (EC; (Nusinow *et al.*, 2011)), which inhibits transcription of *PRR* genes at late night and early morning, thus enabling re-activation of *CCA1* and *LHY*, starting a new cycle (Dixon *et al.*, 2011, Helfer *et al.*, 2011, Herrero *et al.*, 2012).

In order to keep time, circadian clocks are synchronized daily to the environmental light/dark cycle by a process called entrainment. The most potent entraining stimulus is light. UV-B, blue, red or far-red light signals absorbed and processed by specialized photoreceptors (Devlin and Kay, 2000, Feher *et al.*, 2011, Wenden *et al.*, 2011) reach the oscillator via the light input pathway and cause a change in the abundance, activity or localization of one or more oscillator components (Hsu and Harmer, 2014). Transcription of *CCA1*, *LHY*, *PRR9* and *ELF4* is positively regulated by light representing a potential mechanism for entrainment. However, the molecular details of this regulation, including the transcription factors mediating the light

response, are poorly understood and were described in the case of *ELF4* so far (Li *et al.*, 2011). Two transposase-derived transcription factors, FAR-RED ELONGATED HYPOCOTYL 3 (FHY3) and FAR-RED IMPAIRED RESPONSE 1 (FAR1) (Lin *et al.*, 2007), were shown to bind specific *cis*-elements of the *ELF4* promoter and positively regulate *ELF4* transcription. The bZIP-type transcription factor ELONGATED HYPOCOTYL 5 (HY5) was also shown to associate with the *ELF4* promoter occupying *cis*-elements different from those of FHY3 and FAR1. HY5 and its only homolog HY5-HOMOLOG (HYH) preferentially bind to the so-called ACGT-Containing Elements (ACEs). The most frequently occurring functional derivatives of ACEs are G- (CACGTG), C- (GACGTC) or Z-boxes (TACGTG), or various hybrids like G/C- (CACGTC), A/C- (TACGTC) or T/G-boxes (AACGTG) (Chattopadhyay *et al.*, 1998, Lee *et al.*, 2007, Binkert *et al.*, 2014). More than thousand genes show altered expression in the *hy5* mutant, and a genome-scale analysis of in vivo binding sites indicated that about 20% of these genes are direct targets of HY5 (Lee *et al.*, 2007). However, HY5 lacks a transcriptional activation/repression domain thus requires co-factors to control gene expression (Ang *et al.*, 1998, Li *et al.*, 2010). HY5 is a master regulator of light signal transduction pathways initiated by all main photoreceptors absorbing photons from the UV-B to the far-red region of the spectrum (Huang *et al.*, 2014). The function/activity of HY5 is regulated by light at multiple levels. First, transcription of *HY5* is induced by light and HY5, HYH, CALMODULIN 7 (CAM7) and B-BOX DOMAIN PROTEIN 21 (BBX21) appear to contribute to this induction via direct binding to the *HY5* promoter (Abbas *et al.*, 2014, Binkert *et al.*, 2014, Xu *et al.*, 2016). Second, light stabilizes HY5 by inhibiting the function of the CONSTITUTIVE PHOTOMORPHOGENIC 1-SUPPRESSOR OF PHYA-105 1-4 (COP1-SPA1-4) ubiquitin ligase complex, which promotes turnover of HY5 and other positive regulators of photomorphogenesis in darkness (Huang *et al.*, 2014, Lu *et al.*, 2015, Sheerin *et al.*, 2015). Third, light inhibits phosphorylation of HY5 that increases the physiological activity of the protein, but also affects its COP1-mediated degradation (Hardtke *et al.*, 2000).

The role of HY5/HYH in the regulation of the circadian clock has been tested by several studies with variable results (Andronis *et al.*, 2008, Feher *et al.*, 2011);(Li *et al.*, 2011). These authors monitored the function of the clock in *hy5* mutants free-running in continuous white light and found either short period rhythms or no significant period changes even though transcription rate of *ELF4:LUC* was severely attenuated by the absence of HY5/HYH. We reasoned that the spectral composition of white light could have been different among the different studies that may account for the observed variations of results. In order to clarify the circadian clock-related function of HY5 and its homolog HYH, we monitored rhythmic expression of various clock-

controlled luciferase markers and clock genes in *hy5*, *hyh* and *hy5 hyh* mutant backgrounds in different monochromatic light conditions. We found that HY5/HYH mediated signalling to the clock is most pronounced in blue light. Our results suggest that blue light positively regulates accumulation of HY5/HYH via transcriptional and post-transcriptional mechanisms. Red light has a similar, but less efficient effect explaining the blue-enhanced phenotypes. We demonstrate that HY5 binds to the promoters of almost all clock genes in vitro and in vivo and that light modulates this association via regulating HY5 protein levels. Although expression profiling of the *hy5 hyh* mutant showed altered transcription of three clock genes (*PRR5*, *LUX* and *BOA*) only, mathematical modelling indicated that HY5 probably affects the expression of additional oscillator components as well. Our data collectively suggest that HY5/HYH mediates blue light signalling to the clock via direct transcriptional regulation of clock genes.

RESULTS

HY5 and HYH affect the pace of clock in light-dependent manner

Several previous works addressed - either directly or indirectly - the clock-related function of the HY5 transcription factor, but their findings were variable reporting stronger or weaker short period phenotypes for *hy5* mutants or even the lack of any period phenotypes (Andronis *et al.*, 2008, Feher *et al.*, 2011, Li *et al.*, 2011, Haydon *et al.*, 2013). We noticed that all these studies used continuous white light (WL) during free-running, that presumably kept all main visible light-absorbing photoreceptors activated. HY5 is capable of mediating signalling from all of these receptors, but obviously, light signals can reach the oscillator via HY5-dependent and –independent pathways. However, if the supposed HY5-dependent light signalling route to the clock is selectively enhanced/repressed by particular wavelengths of light, the possible variation in the spectral composition of the different white light sources could explain the apparently divergent behaviour of the clock in *hy5* mutants. This prompted us to test the circadian function of HY5 and its close homolog, HYH in continuous monochromatic blue (BL), red (RL) and far-red (FRL) light conditions.

To facilitate monitoring of circadian rhythms, the *CHLOROPHYLL A/B-BINDING PROTEIN 2* (*CAB2*)*:LUC* reporter construct (Hall *et al.*, 2001) was introgressed into *hy5-ks50* (*hy5*), *hyh-1* (*hyh*) and *hy5-ks50 hyh-1* (*hy5 hyh*) double mutant plants. According to our standard protocol for *in vivo* luciferase imaging (Southern *et al.*, 2006), plants were entrained to 12 h white light (15 µmol m^{-2} s^{-1})/ 12 h dark (12:12 LD) photocyles for 7 days, then transferred to continuous white light (WL), where luminescence was monitored for 5 to 7 days. Figure 1A shows the rhythmic expression of the *CAB2:LUC* marker in the different genetic backgrounds. Period

estimates indicated short period phenotypes for *hy5* and *hy5 hyh* mutants (Fig. 1B, WL). Next, the measurements were repeated on plants transferred to BL or RL at equal fluence rates (15 µmol m^{-2} s^{-1}) (Fig.1B, BL and RL, respectively) or to FRL light at 5 µmol m^{-2} s^{-1} fluence rate (Fig.S1). In BL *hy5* and *hy5 hyh* showed marked short period phenotypes. In contrast to WL conditions, the *hyh* single mutants in BL produced shorter periods compared with WT plants (Fig.1B, BL). The results in RL largely resembled those in WL, but the phenotypes were weaker. The *hy5* and *hy5 hyh* mutants showed faint short period phenotypes, whereas the *hyh* single mutant behaved like WT (Fig.1B, RL). In FRL, however, the amplitude of *CAB2:LUC* rhythms was severely reduced so that estimation of periods was not possible (Fig.S1).

In order to test if HY5 and HYH influence the rhythmic expression of core clock genes and output components in addition to *CAB2*, the *CIRCADIAN CLOCK ASSOCIATED 1 (CCA1):LUC*, *GIGANTEA (GI):LUC* and *COLD- AND CIRCADIAN-REGULATED 2 (CCR2):LUC* reporters were introgressed in the mutant backgrounds. Plants were entrained as above and were transferred to continuous BL, RL, FRL or darkness (DD) after entrainment. Figure 1C demonstrates that expression of *CCA1:LUC*, *GI:LUC* and *CCR2:LUC* displayed period phenotypes very similar to that of *CAB2:LUC*. Stronger or weaker short period phenotypes were observed in the *hy5* and *hy5 hyh* mutants in BL or RL, respectively. The *hyh* mutant showed very mild short periods for all reporters in BL only. In DD, very weak short period phenotypes were detected in the *hy5* and *hy5 hyh* mutants only. In FRL, strong dampening of rhythmic LUC activity prevented reliable calculation of periods. Collectively these data suggest that HY5 and HYH are components of the circadian light input pathway and they affect the oscillator mainly in blue light.

HY5 is associated with the promoters of most clock and clock-associated genes preferably in blue light

To identify clock genes bound by HY5 differentially in BL and RL, a ChIP-seq (chromatin immunoprecipitation followed by deep sequencing) assay was performed (Methods S1) using plants that expressed the HY5-YFP fusion protein under the control of the native HY5 promoter in the *hy5* mutant background. Plants entrained to 12:12 LD cycles were transferred to BL or RL for 52 h and chromatin was precipitated using an anti-GFP antibody. Reads were mapped against the full annotated genome of *Arabidopsis thaliana* and loci corresponding to the 5' regulatory region of protein coding genes and showing significant (more than 4-fold) enrichment over the mock control were identified (Data S1). Around 7000 and 3500 genes were identified in BL and RL respectively (Fig.2A). Note that essentially all the genes that were

bound by HY5 in RL were included in the BL gene set as well. The combined BL+RL gene list showed significant overlap with the HY5-bound genes identified by Lee and co-workers (Lee et al., 2007) despite the different assay conditions and detection method (Fig.2B). In agreement with this, the distribution of gene ontology (GO) categories showed very similar patterns in the two studies (Fig. S2). GO enrichment analysis indicated that genes related to circadian rhythmicity were overrepresented in the BL+RL gene list, as were the genes related to well-established functions of HY5, such as UV-B and osmotic/salt stress signalling (Table S1). Accordingly, Figure 2B also demonstrates that the majority (26 out of 34) of clock and clock-associated genes (Hsu and Harmer 2014) showed association with HY5 in the present work, whereas 13 of these were included in the Lee 2007 dataset. These data suggested that binding of HY5 to genomic targets is enhanced in BL and that HY5 is associated with most of the clock and clock-associated genes in vivo. Fold enrichment values in BL and RL conditions for all HY5-bound genes (Fig.2C) and for the clock genes (Fig.2D) were plotted to support the enhanced binding of HY5 in BL with quantitative data. Moreover, Figure S3 indicates that genes that show weak HY5 binding in BL are rarely detected in the RL gene set, whereas loci with strong association to HY5 in BL are usually bound in RL as well. Collectively these data suggest quantitative, but not qualitative differences between the BL and RL gene lists. In other words, occupation of target promoters by HY5, including those of the clock genes, is generally enhanced in BL compared to RL, but the binding specificity is apparently unaffected by light quality.

In order to validate the light-dependent modulation and to test potential temporal regulation of HY5 binding, entrained *HY5:HY5-YFP* plants were transferred to BL and RL and samples were harvested at 48 h and 60 h after the transfer, then ChIP was performed as above. These time points (ZT 48 and ZT 60) correspond to the peak times of morning- and evening-phased genes and mark two opposite points of the circadian cycle. Primers located within the genomic regions identified by ChIP-seq for *CCA1*, *PRR9*, *PRR5*, *LUX*, *ELF3*, *ELF4* and *TOC1* were used to test precipitated DNA samples by qPCR assays. Figure 3 demonstrates that occupation of all tested promoters by HY5 is clearly enhanced in BL compared with RL, thus validating the ChIP-seq results. On the other hand, HY5 was present at very similar levels at ZT 48 and ZT 60 at all tested loci, indicating that association of HY5 with the target promoters is not controlled by the clock.

HY5 binds to conserved *cis*-acting elements of clock gene promoters in vitro

Modulation of gene expression by HY5 mostly involves the formation of protein-DNA complexes between HY5 and specific *cis*-elements with the core sequence of ACGT (ACGT-containing element, ACE). Indeed, *de novo* motif-finding identified the ACGT core sequence and an associated nearly complete G-box motif in half of the target regions (Figure S4). Figure 4A shows examples of different ACE/(G-box)-variants present in the proximal regions of *CCA1*, *PRR9*, *PRR5*, *LUX*, *ELF3, ELF4* and *TOC1* promoters identified by ChIP-Seq assays. Direct binding of HY5 to the ACE(s) of *ELF4* has been reported (Li *et al.*, 2011). In order to test the ability of HY5 to specifically bind to the other variants in their native sequence contexts, Electrophoretic Mobility Shift Assays (EMSAs) were performed. Each probe represented a short region of the corresponding promoter carrying either wild-type (W) or mutated (M) version of a single G-box or G-box-like element (Fig.4A and Table S2). Note that the *PRR5*, *LUX* and *ELF4* probes carried two closely located elements. The results of EMSA showed that bacterially expressed recombinant HY5 proteins could bind to each of the probes, except for *ELF3* ACE, indicating that the core ACGT sequence must be flanked at least one C or G nucleotide in order to mediate HY5-binding (Fig.4B). Mutations in the ACE elements prevented the formation of HY5-DNA complexes in each case, demonstrating that the binding was mediated specifically via these *cis*-elements. These data demonstrate the capability of HY5 to bind directly to specific elements of clock gene promoters in vitro.

HY5 and HYH levels are increased in blue light

The increased chromatin-association of HY5 in BL compared with RL, could be explained by elevated expression of HY5 and HYH specifically in BL conditions. The mRNA abundance of *HY5* and *HYH* was tested in WT plants grown in 12:12 LD cycles for 7 days and then transferred to BL or RL and samples were harvested at the times indicated (Fig.5A, B). Both mRNA species showed clear oscillations and were significantly higher in BL compared with RL (Fig.5A, B). The positive effect of BL was more pronounced on *HYH* mRNA levels. To monitor HY5 and HYH protein levels, HY5-YFP or HYH-YFP fusion proteins were expressed under the control of native (*HY5:HY5-YFP* or *HYH:HYH-YFP*) or the strong constitutive *35S* promoter (*35S:HY5-YFP* or *35S:HYH-YFP*) in the corresponding *hy5* or *hyh* mutant backgrounds. Functionality of the fusion proteins was verified by full complementation of the photomorphogenic phenotypes of *hy5* and *hyh* mutants (Fig.S5). In the *HY5:HY5-YFP* and *HYH:HYH-YFP* lines, HY5-YFP and HYH-YFP fusion proteins were clearly detectable in BL (Fig.5C, E). HYH-YFP levels showed clear oscillations corresponding to the rhythm at mRNA

level, but no significant temporal changes were observed for HY5-YFP accumulation (Fig. S6). In RL, HY5-YFP levels decreased and HYH-YFP was hardly detectable compared with BL conditions (Fig.5C, E). In the *35S:HY5-YFP* and *35S:HYH-YFP* lines, neither HY5-YFP nor HYH-YFP protein levels showed any oscillations, as expected. Importantly, despite the light-independent transcriptional activity of the *35S* promoter, the level of both fusion proteins was lower in RL compared with BL condition (Fig.5D, F). These data demonstrate that HY5-YFP and HYH-YFP proteins accumulate to a higher level in BL compared with RL of identical photon fluence rate and that BL stimulates HY5/HYH accumulation at both transcriptional and post-transcriptional levels. In agreement with earlier results, our data also show that relative to darkness, RL promotes the accumulation of HY5 (Fig.5C, D).

HY5 and HYH regulate the expression of core clock genes

To reveal the actual effect of HY5/HYH on the transcription of targeted clock genes, mRNA levels of all clock or clock-associated genes (Hsu and Harmer) that were bound by HY5 in BL (26 genes, Fig.2D) were determined in WT (Ws) and *hy5 hyh* mutant seedlings in BL (Fig.6 and Fig.S7). Consistent with the basic circadian phenotype observed before (Fig.1), all rhythmic genes were expressed with a short period rhythm in the *hy5 hyh* mutant in BL; however, only three of them (*PRR5*, *LUX* and *BOA*) showed significantly altered (increased) mean expression levels. These genes, along with the non-changing *CCA1* were also tested in RL. Intriguingly, neither the expression pattern nor the level of these genes were affected in the *hy5 hyh* mutant in RL conditions. These data might indicate that HY5 affects the clock via the transcriptional repression of *PRR5*, *LUX* and *BOA*, despite binding to the promoters of many other clock genes.

Modelling of the clock in *hy5 hyh* mutants suggests that HY5 affects transcription of other clock genes, in addition to *PRR5*, *LUX* and *BOA*

The function of the clock relies on the intricate network of cross-regulation among clock genes and clock proteins, resulting in rhythmic but well-established mean expression levels of clock components. Mathematical models, based on the identified regulatory links and a given sets of parameters in order to fit experimental data, have been constructed and can be used to predict how the function (period, phase, amplitude) of the oscillator is altered in response to changes of clock gene expression. This prompted us to test if the observed increase in the mean expression of *PRR5*, *LUX* and *BOA* in the *hy5 hyh* mutant is consistent with the short period phenotype. We used the recent model by de Caluwé for this analysis (De Caluwe *et al.*,

2016)(Methods S1). This model is based on the network of eight clock genes that have been grouped in four functional units: P51 (PRR5, TOC1), CL (CCA1, LHY), P97 (PRR7, PRR9) and EL (ELF4, LUX). Simulation of the de Caluwé model using default parameters (representing WT behaviour) resulted in 23.44h period of oscillations (Fig. 7A). In order to test the clock behaviour in the *hy5 hyh* mutant (Fig. 6), effects of changes to all transcription rate parameters were investigated.

In accordance with our data and the predicted effects on transcription parameter changes on behaviour of P51 and EL (Fig. S9), it was assumed that at least transcription rate constants of P51 and EL would be increased. Model scaled period derivatives and scaled solution partial derivatives indicate that this will lead to an increase in the period, as well as an increase in the levels of all four transcripts: P51, EL, CL and P7/9 (Fig. S8 and S9). An actual increase of 50% of transcript rates validated this approximation (Fig. 7B) with levels of all raised and the period increased. Thus to provide a better qualitative fit to most of the mutant phenotype, the model predicts that other parameters would have to be changed. Doubling the transcription rate parameters (CL dependent and independent one) of P97 (Fig. 7C and 7D) will shorten the period and lower the levels of CL and P79, giving a closer match to the data. In the model, the transcription of P97 is negatively affected by P51 and EL. Lowering transcription rate of P97 will lower levels of *CCA1*, but will also increase levels of P51 and EL mRNA. This can be seen from the predicted effect of scaled solution derivatives of P51 and EL mRNA time series with respect to v_{2A} and v_{2B} (Fig. S9). An increase in the latter two genes will lead to an overall decrease in the level of P97 mRNA, despite an increase in the transcription rate constant. The period can be further decreased by increasing those rates further (Fig. 7E). Decreasing the transcription rate of CL (Fig. 7F) by 50% will have a similar improvement to the fit of CL and lead to a period shortening, though P97 level will be less well fit. Combination of an increase CL-dependent in P97 transcription and decrease in CL transcription (and further larger changes) will have a similar effect (Fig. 7G and 7H).

On one hand, these results indicate that this reduced model qualitatively predicts most of the mutant phenotype if only a handful of transcription rates are affected. On the other hand, these data may suggest that transcription of certain clock genes (e.g. *CCA1* or *PRR9*) could be directly regulated by HY5 even if expression levels of those genes are apparently not altered in the *hy5 hyh* mutant. We hypothesised that in these cases, the loss of HY5 function does affect gene expression, but this is compensated by other clock components that are also targeted by HY5; so that this complex regulation would result in an apparently WT-like expression level in the *hy5 hyh* mutant.

DISCUSSION

Synchronizing the circadian clock with the environment is essential to ensure that clock-controlled events occur at the appropriate times of the day. Modulation of clock gene expression by light is a common mechanism for this process, not only in plants, but in other eukaryotic organisms as well (Harmer *et al.*, 2001). Previous studies suggested that HY5, a key transcription factor of general light signalling cascades, could be involved in this process, although the results were rather variable. Some authors demonstrated that loss of HY5 function causes short period rhythms (Andronis *et al.*, 2008, Haydon *et al.*, 2013), whereas others reported no obvious period phenotypes for *hy5* mutants (Feher *et al.*, 2011, Li *et al.*, 2011). This apparent contradiction has not been addressed until now.

Here we showed that in blue light *hy5* and *hyh* mutants produce rhythms with notably shorter periods compared to WT plants, but in red light the phenotype is hardly detected. The mutants displayed an intermediate phenotype in white light suggesting that the ratio blue and red wavelengths is an important determinant of the actual effect of HY5 and HYH on the clock. Thus the discrepancy in previous results on the circadian function of HY5 and HYH could be caused by the variable light conditions.

Our transcript profiling data linked these phenotypes to the altered expression of clock genes in the *hy5 hyh* mutant. We found that *PRR5*, *LUX* and *BOA* showed elevated mRNA levels in the mutant specifically in blue light. However, modelling of the clock in *hy5 hyh* mutants (i.e. increased transcription of *PRR5*, *LUX* and *BOA*) predicted a long period phenotype, which is the opposite of the observed effect. The same model predicted elevated *CCA1* mRNA levels, which were not detected in the *hy5 hyh* mutant in any conditions. Intriguingly, when *CCA1* mRNA levels were set to WT-like levels in the mutant, the simulation gave periods shorter than in the WT. This scenario could be explained if a direct positive effect of HY5 on *CCA1* expression is balanced out by negative feed-back effects from other clock components that are also directly targeted by HY5. This would support our hypothesis on a more general regulatory role of HY5 within the circadian system. Evidently, our data do not represent direct evidences, but are consistent with this hypothesis. Experimental testing of our assumption and the validation of direct primary clock gene targets of HY5 will require further work and methods enabling stringent inducible ectopic expression of HY5 and subsequent kinetic analysis of clock gene expression (Gendron *et al.,* 2012, Adams *et al.* 2015).

Nevertheless, our results combined with modelling highlight the fact that the specific effect (activation or repression) of a transcription factor (TF) on individual components of a highly interconnected gene network may not be concluded correctly from the analysis of TF mutant

plants, especially if the TF directly binds to several components of the network. Thus, our study indicates that high throughput and large scale experimental approaches are necessary but not sufficient *per se* to decipher the structure and mechanistic details of complex systems and instead of intuitive explanation attempts, mathematical modelling is required for correct interpretation of such data.

Since HY5 does not possess a transcriptional activation domain (Ang *et al.*, 1998, Li *et al.*, 2010), it requires co-factors to regulate transcription of target genes. For instance, FAR-RED ELONGATED HYPOCOTYL 3 (FHY3), a transposase-derived transcription factor binds to the *ELF4* promoter in vivo and is essential for *ELF4* transcription (Li *et al.*, 2011). FHY3 physically interact with HY5 suggesting that FHY3 could act as a co-factor of HY5 controlling *ELF4*. FHY3 also directly binds to the *CCA1* promoter (Lin *et al.*, 2007, Li *et al.*, 2011) indicating another potential clock gene target for the FHY3-HY5 complex. HY5 and HYH were shown to physically and functionally interact with several B-BOX DOMAIN PROTEINs (Gangappa and Botto, 2016) and with PHYTOCHROME INTERACTING FACTOR 1 and 3 (Chen *et al.*, 2013). However, the function of these interactions was linked so far to the regulation of photomorphogenesis and reactive oxygen species signalling, but not to the control of the circadian clock.

The mechanisms by which HY5 represses transcription involve inhibition of binding and/or the activity of a positive transcription factor (Li *et al.*, 2010), promotion of repressive histone methylation, or even direct transcriptional repression (Jing *et al.*, 2013). In addition, HY5 was shown to interact with CCA1 in yeast (Andronis *et al.*, 2008). Thus it is possible that HY5 interferes with DNA-binding or function of CCA1, which is now considered to act as a general transcriptional repressor within the circadian system (Kamioka *et al.*, 2016). Interestingly, Evening Elements, mediating DNA-binding of CCA1 are found in the promoters of *PRR5*, *LUX* and *BOA* relatively close to the binding sites of HY5. This could allow simultaneous DNA-binding and interaction of HY5 and CCA1 to modulate expression of these clock genes.

We showed that the blue light-enhanced circadian phenotype of *hy5 hyh* mutants is accompanied by increased association of HY5 with the promoters of clock genes. We also provided evidence that accumulation of HY5 and HYH is promoted by blue light much more than by red light, at both transcriptional and post-transcriptional levels. It is likely that enhanced binding of HY5 to the promoters in blue light is a result of higher levels of HY5 proteins under these conditions, although contribution of blue light induced modification(s) of HY5 cannot be excluded. Recent data indicate that intricate complexes of transcription factors, including HY5 and HYH, are associated with the promoters of clock genes (Li *et al.*, 2011, Kamioka *et al.*,

2016). Our data suggest that the amount of HY5/HYH in these complexes may dynamically change according to the ratio of blue and red components of light, representing a potential mechanism how light quality, in addition to light quantity, modulates the function of the plant circadian clock.

EXPERIMENTAL PROCEDURES

Plant materials, growth conditions and light treatments

All plants used in this work were of the Wassilevskija (Ws) accession of *Arabidopsis thaliana*. The *hy5-ks50* and *hyh-1* mutants and the *hy5-ks50 hyh-1* double mutant have been described (Oyama *et al.*, 1997, Holm *et al.*, 2002, Feher *et al.*, 2011). These mutants are referred to as *hy5*, *hyh* or *hy5 hyh* in the text. The *CAB2:LUC*, *CCR2:LUC*, *CCA1:LUC* and *GI:LUC* reporter constructs have been described (Hall *et al.*, 2001, Doyle *et al.*, 2002, Palagyi *et al.*, 2010). These constructs were transformed in wild-type Ws plants (Clough and Bent, 1998). Homozygous single-copy T3 lines were selected for each construct and crossed to *hy5 hyh* plants in order to have the same copy of a particular marker gene in all genetic backgrounds.

To produce the *35S:HY5-YFP* and *35S:HYH-YFP* gene constructs, *HY5* and *HYH* cDNA molecules without the translational termination codons were PCR-amplified from a size-selected cDNA library (CD4-13, TAIR) and cloned as *BamH*I-*Sma*I fragments between the *35S* promoter of the Cauliflower Mosaic Virus and the *Yellow Fluorescent Protein* (*YFP*) gene in the modified pPCV812 binary vector (Bauer *et al.*, 2004). To create the *HY5:HY5-YFP* and *HYH:HYH-YFP* constructs, the promoter regions of *HY5* and *HYH* were PCR amplified first. These fragments contained the full 5' UTR regions, but not the ATG and were 756 bp (*HY5*) or 2302 bp (*HYH*) long. Next, the *35S* promoter in the *35S:HY5-YFP* and *35S:HYH-YFP* constructs was excised by *Hind*III-*Xba*I digestion and replaced by *HY5* (*Hind*III-*Stu*I) or *HYH* (*Hind*III-*Spe*I) promoter fragments. For all assays surface sterilized seeds were sown on solidified Murashige and Skoog (MS) media supplemented with 0.5 % (w/v) sucrose. White light during growth/entrainment was provided by LUMILUX XT T8 L 36 W/865 (Osram) fluorescent tubes at 70-100 μmol m^{-2} s^{-1} fluence rate, whereas during free-run TUNSGRAM 15W F33-640 cool white tubes (General Electric) were operated at 15 μmol m^{-2} s^{-1} fluence rate. Red (λ_{max} = 660 nm), far-red (λ_{max} = 735 nm) and blue light (λ_{max} = 470 nm) were provided by SNAP-LITE LED light sources (Quantum Devices, WI, USA).

Analysis of gene expression

Plants were grown for 10 days in the indicated photocycles before harvesting. Total RNA was isolated with the NucleoSpin® RNA Plant Kit (Macherey-Nagel, #740949). 1 µg RNA was used as template for reverse transcription done with the RevertAid RT Reverse Transcription Kit (Thermo Scientific, #K1691). All procedures were performed according to the manufacturer's instructions. cDNA samples were diluted 1:5 and the amount of 1.5 µl was used in 20 µl reaction volume in quantitative real-time PCR (qPCR) assays employing Power SYBR® Green Master Mix (Applied Biosystems, #4368702) and an ABI Prism 7300 Real Time PCR System (Applied Biosystems). qPCR primers were designed using PerlPrimer v1.1.21 and their specificity was checked by Primer-BLAST (https://www.ncbi.nlm.nih.gov/tools/primer-blast/). Primers with melting points of 59ºC-61ºC were designed to produce amplicons of 80-150 base pairs. One of each primer pairs was designed to span an exon/intron boundary, except for intron-less genes, such as *ELF4*. Final concentration of primers was 300 nM. Running parameters for ABI Prism 7300 were as follows: initial denaturation and activation of the polymerase: 95ºC for 2 min; 40 cycles of denaturation at 95ºC for 15 s and annealing/extension at 60ºC for 1 min, where SYBR Green fluorescence was determined during the annealing/extension step. ROX was employed as a passive dye. After completing 40 cycles of amplification, dissociation curves were determined that indicated the presence of a single amplified product in the reaction mixture for any given primer pairs. The standard curve method was used for calculation of relative expression levels. Spare samples of WT plants harvested in BL between 24h and 48h of the free-run (9 samples in total) were processed as above, but the resulted cDNA samples were joined and then used to make ten-fold dilutions in order to produce standard series of four different cDNA concentrations, including the starting non-diluted one. The same standard series was included in all runs during the project that makes the expression levels of a given gene in different conditions comparable. Expression values relative to the standard were normalised to *TUBULIN 2/3* (TUB) mRNA levels. Accumulation of *TUB 2/3* mRNA showed no circadian patterns under the conditions used (Fig.S10).

Total protein extraction, electrophoretic separation and blotting of total protein samples were done essentially as described (Kevei *et al.*, 2007). To detect YFP fusion proteins, the Living Colors® A.v. monoclonal (JL-8) mouse antibody (Takara Bio Clontech, #632380) was used at 1:2000 dilution. Actin proteins (isoforms ACT1, 2, 3, 4, 7, 8, 11 and 12) were detected by the monoclonal (10-B3) Anti-Actin (plant) mouse antibody at 1:10000 dilution (Sigma, #A0480). As for the secondary antibody, a horse radish peroxidase-conjugated anti-mouse goat antibody

(Thermo Scientific, #31431) was used at 1:10000 dilution. Chemiluminescent signals were detected and visualized as described (Medzihradszky *et al.*, 2013). The assays were repeated two or three times and representative data are shown.

Luminescence assays

Luciferase activity was measured by measuring single seedlings with an automated luminometer (TopCount NXT, Perkin Elmer) for 7 days as described previously (Kevei *et al.*, 2006). All rhythm data were analysed with the Biological Rhythms Analysis Software System (BRASS, available at http://www.amillar.org), running fast Fourier transform nonlinear least-squares estimation. Variance-weighted mean periods within the circadian range (15–40 h) and SEMs were estimated as described, from 10 to 36 traces per genotype. Experiments were repeated three or four times.

Electrophoretic Mobility Shift Assays (EMSAs)

Double-stranded probes were produced by annealing complementary oligonucleotides (IDT) in 10 mM Tris-HCl (pH 7.5), 1 mM EDTA, 50mM NaCl. Equal amounts of complementary oligos were mixed at a final concentration of 40 µM, heated to 95 ^{o}C for 5 min in a block heater and let to cool down to RT overnight. The 5' end of the forward oligonucleotide was labelled by biotin (IDT). HY5 proteins with an N-terminal 6xHis tag were expressed in *E. coli* BL21 cells and purified using Ni-NTA agarose matrix (Qiagen). Protein expression and purification was done according to the manufacturer's instructions (Qiagen, QIAexpressionist). Binding reactions contained 10mM Tris-HCL pH 7.5, 85 mM KCl, 5% (v/v) glycerol, 0.1 µg/µl poly (dI•dC), 40 fmol probe and 100 ng of purified HY5 proteins in 20 µl volume. Reactions were incubated at RT for 20 and loaded on native 4% polyacrylamide gels made with 0.5x TBE buffer. Gels were run in 0.5x TBE for 70 min and electro-blotted to Hybond-N+ (Amersham) nylon membrane in 0.5x TBE for 60 min. Detection of biotin-labelled fragments was done using the Chemiluminescent Nucleic Acid Detection Module (Thermo Scientific) according to the manufacturer's protocols. Chemiluminescent signals were detected as for the Western-blots.

Chromatin Immunoprecipitation (ChIP) assays

The ChIP protocol by Werner Aufsatz (http://www.epigenome-noe.net/researchtools/protocol.php?protid=13) was applied with the following modifications. Ten-day-old plants were fixed in 1 % (v/v) formaldehyde solution. Chromatin samples were sonicated on ice six times for 10 s using a Vibra Cell sonicator (SONICS & MATERIALS Inc.,

Danbury, CT, USA) at 10% power. Sonicated and diluted chromatin samples were pre-cleared by 20 µl (bed volume) of binding control agarose beads (Chromotek GmbH, Germany) for 1 h at 4°C. An aliquote of the pre-cleared chromatin solution was saved for the input sample and the rest of the material was precipitated using 12.5 µl (bed volume) of GFP-Trap agarose beads (Chromotek GmbH, Germany) for 16 h at 4°C. Precipitated chromatin was eluted from the beads, and along with the input sample, it was de-crosslinked and DNA was extracted using the NucleoSpin® Gel and PCR Clean-up kit (Macherey-Nagel, 740609) with Buffer NTB (Macherey-Nagel, 740595). The final volume of purified DNA samples was about 45 µl. Volume of 1.5 µl of the eluate was analysed in qPCR reactions with reaction parameters and conditions described for the analysis of gene expression. Primers were designed to amplify genomic regions around the putative HY5 binding sites. Standard series were prepared from ten-fold dilutions of the input DNA samples. The control (mock) sample was produced from BL-treated by executing the same steps as above, but instead of GFP-Trap agarose beads, control agarose beads (i.e. without the immobilized anti-GFP antibody) were used for precipitation. ChIP-related qPCR primers are listed in Table S2. ChIP data were analyzed and presented according to the "percent of input" method (Haring *et al.*, 2007).

For details on ChIP-Seq analysis and mathematical modelling please see Methods S1. Raw ChIP-Seq data (i.e. reads) have been deposited at the NCBI GEO repository under the accession number GSE117797 (https://www.ncbi.nlm.nih.gov/geo/query/acc.cgi?acc=GSE117797).

ACKNOWLEDGEMENTS

We are grateful to Gabriella Veres and Györgyi Sándor for excellent technical assistance. This work was supported by the Hungarian Scientific Research Fund (grant no. K-106361 to L.K.-B. and grant nos. K-108559, GINOP-2.3.2-15-2016-00001 and GINOP-2.3.2-15-2016-00015 to F.N.), and by a Research Chair Award from the Scottish Universities Life Science Alliance to F.N.

The authors declare that they do not have any conflicts of interest.

SUPPORTING INFORMATION

Figure S1. Low-amplitude rhythms of the *CAB2:LUC* reporter in continuous far-red light

Figure S2. Distribution of functional (GO) categories within the HY5-bound genes

Figure S3. BL and RL gene lists are quantitatively different

Figure S4. Top five de novo motif finding results from Homer.

Figure S5. Complementation of the photomorphogenic phenotypes of *hy5* and *hyh* mutants by HY5-YFP and HYH-YFP proteins

Figure S6. Non-rhythmic accumulation of the HY5-YFP fusion protein in continous blue light

Figure S7. Clock or clock-associated genes showing unaltered mean expression levels in the *hy5 hyh* mutant versus WT in BL

Figure S8. Simulated mRNA levels over one cycle and scaled solution derivatives.

Figure S9. Barplot of the scaled period sensitivity coefficients of the model transcription rates.

Figure S10. mRNA accumulation of *TUBULIN 2/3* shows no circadian patterns under the conditions used in this work

Table S1. Gene Ontology Enrichment analysis of the combined BL+RL gene lists by PANTHER13 (Mi *et al.*, 2013, Mi *et al.*, 2017)

Table S2. Primers and oligonucleotides used in qPCR, ChIP qPCR and EMSA assays

Data S1. List of genes bound by HY5 in BL and RL.

Methods S1. Description of ChIP-Seq analysis and mathematical modelling.

REFERENCES

Abbas, N., Maurya, J.P., Senapati, D., Gangappa, S.N. and Chattopadhyay, S. (2014) Arabidopsis CAM7 and HY5 physically interact and directly bind to the HY5 promoter to regulate its expression and thereby promote photomorphogenesis. *Plant Cell*, **26**, 1036-1052.

Adams, S., Manfield, I., Stockley, P. and Carre, I.A. (2015) Revised Morning Loops of the Arabidopsis Circadian Clock Based on Analyses of Direct Regulatory Interactions. *PLoS One*, **10**, e0143943.

Andronis, C., Barak, S., Knowles, S.M., Sugano, S. and Tobin, E.M. (2008) The clock protein CCA1 and the bZIP transcription factor HY5 physically interact to regulate gene expression in Arabidopsis. *Mol Plant*, **1**, 58-67.

Ang, L.H., Chattopadhyay, S., Wei, N., Oyama, T., Okada, K., Batschauer, A. and Deng, X.W. (1998) Molecular interaction between COP1 and HY5 defines a regulatory switch for light control of Arabidopsis development. *Mol Cell*, **1**, 213-222.

Bauer, D., Viczian, A., Kircher, S., Nobis, T., Nitschke, R., Kunkel, T., Panigrahi, K.C., Adam, E., Fejes, E., Schafer, E. and Nagy, F. (2004) Constitutive photomorphogenesis 1 and multiple photoreceptors control degradation of phytochrome interacting factor 3, a transcription factor required for light signaling in Arabidopsis. *Plant Cell*, **16**, 1433-1445.

Baudry, A., Ito, S., Song, Y.H., Strait, A.A., Kiba, T., Lu, S., Henriques, R., Pruneda-Paz, J.L., Chua, N.H., Tobin, E.M., Kay, S.A. and Imaizumi, T. (2010) F-box proteins

FKF1 and LKP2 act in concert with ZEITLUPE to control Arabidopsis clock progression. *Plant Cell*, **22**, 606-622.

Binkert, M., Kozma-Bognar, L., Terecskei, K., De Veylder, L., Nagy, F. and Ulm, R. (2014) UV-B-responsive association of the Arabidopsis bZIP transcription factor ELONGATED HYPOCOTYL5 with target genes, including its own promoter. *Plant Cell*, **26**, 4200-4213.

Chattopadhyay, S., Ang, L.H., Puente, P., Deng, X.W. and Wei, N. (1998) Arabidopsis bZIP protein HY5 directly interacts with light-responsive promoters in mediating light control of gene expression. *Plant Cell*, **10**, 673-683.

Chen, D., Xu, G., Tang, W., Jing, Y., Ji, Q., Fei, Z. and Lin, R. (2013) Antagonistic basic helix-loop-helix/bZIP transcription factors form transcriptional modules that integrate light and reactive oxygen species signaling in Arabidopsis. *Plant Cell*, **25**, 1657-1673.

Clough, S.J. and Bent, A.F. (1998) Floral dip: a simplified method for Agrobacterium-mediated transformation of Arabidopsis thaliana. *Plant J*, **16**, 735-743.

De Caluwe, J., Xiao, Q., Hermans, C., Verbruggen, N., Leloup, J.C. and Gonze, D. (2016) A Compact Model for the Complex Plant Circadian Clock. *Front Plant Sci*, **7**, 74.

Devlin, P.F. and Kay, S.A. (2000) Cryptochromes are required for phytochrome signaling to the circadian clock but not for rhythmicity. *Plant Cell*, **12**, 2499-2510.

Dixon, L.E., Knox, K., Kozma-Bognar, L., Southern, M.M., Pokhilko, A. and Millar, A.J. (2011) Temporal repression of core circadian genes is mediated through EARLY FLOWERING 3 in Arabidopsis. *Curr Biol*, **21**, 120-125.

Dodd, A.N., Salathia, N., Hall, A., Kevei, E., Toth, R., Nagy, F., Hibberd, J.M., Millar, A.J. and Webb, A.A. (2005) Plant circadian clocks increase photosynthesis, growth, survival, and competitive advantage. *Science*, **309**, 630-633.

Domijan, M., Brown, P.E., Shulgin, B.V. and Rand, D.A. (2016) PeTTSy: a computational tool for perturbation analysis of complex systems biology models. *BMC Bioinformatics*, **17**, 124.

Doyle, M.R., Davis, S.J., Bastow, R.M., McWatters, H.G., Kozma-Bognar, L., Nagy, F., Millar, A.J. and Amasino, R.M. (2002) The ELF4 gene controls circadian rhythms and flowering time in Arabidopsis thaliana. *Nature*, **419**, 74-77.

Eriksson, M.E., Hanano, S., Southern, M.M., Hall, A. and Millar, A.J. (2003) Response regulator homologues have complementary, light-dependent functions in the Arabidopsis circadian clock. *Planta*, **218**, 159-162.

Feher, B., Kozma-Bognar, L., Kevei, E., Hajdu, A., Binkert, M., Davis, S.J., Schafer, E., Ulm, R. and Nagy, F. (2011) Functional interaction of the circadian clock and UV RESISTANCE LOCUS 8-controlled UV-B signaling pathways in Arabidopsis thaliana. *Plant J*, **67**, 37-48.

Fogelmark, K. and Troein, C. (2014) Rethinking transcriptional activation in the Arabidopsis circadian clock. *PLoS Comput Biol*, **10**, e1003705.

Foo, M., Somers, D.E. and Kim, P.J. (2016) Kernel Architecture of the Genetic Circuitry of the Arabidopsis Circadian System. *PLoS Comput Biol*, **12**, e1004748.

Gangappa, S.N. and Botto, J.F. (2016) The Multifaceted Roles of HY5 in Plant Growth and Development. *Mol Plant*, **9**, 1353-1365.

Gendron, J.M., Pruneda-Paz, J.L., Doherty, C.J., Gross, A.M., Kang, S.E. and Kay S.A. (2012). Arabidopsis circadian clock protein, TOC1, is a DNA-binding transcription factor. *Proc Natl Acad Sci U S A*, **109,** 3167–3172.

Greenham, K. and McClung, C.R. (2015) Integrating circadian dynamics with physiological processes in plants. *Nat Rev Genet*, **16**, 598-610.

Hall, A., Kozma-Bognar, L., Toth, R., Nagy, F. and Millar, A.J. (2001) Conditional circadian regulation of PHYTOCHROME A gene expression. *Plant Physiol*, **127**, 1808-1818.

Hardtke, C.S., Gohda, K., Osterlund, M.T., Oyama, T., Okada, K. and Deng, X.W. (2000) HY5 stability and activity in arabidopsis is regulated by phosphorylation in its COP1 binding domain. *EMBO J*, **19**, 4997-5006.

Haring, M., Offermann, S., Danker, T., Horst, I., Peterhansel, C. and Stam, M. (2007) Chromatin immunoprecipitation: optimization, quantitative analysis and data normalization. *Plant Methods*, **3**, 11.

Harmer, S.L., Panda, S. and Kay, S.A. (2001) Molecular bases of circadian rhythms. *Annu Rev Cell Dev Biol*, **17**, 215-253.

Haydon, M.J., Mielczarek, O., Robertson, F.C., Hubbard, K.E. and Webb, A.A. (2013) Photosynthetic entrainment of the Arabidopsis thaliana circadian clock. *Nature*, **502**, 689-692.

Hazen, S.P., Schultz, T.F., Pruneda-Paz, J.L., Borevitz, J.O., Ecker, J.R. and Kay, S.A. (2005) LUX ARRHYTHMO encodes a Myb domain protein essential for circadian rhythms. *Proc Natl Acad Sci U S A*, **102**, 10387-10392.

Heinz, S., Benner, C., Spann, N., Bertolino, E., Lin, Y.C., Laslo, P., Cheng, J.X., Murre, C., Singh, H. and Glass, C.K. (2010) Simple combinations of lineage-determining transcription factors prime cis-regulatory elements required for macrophage and B cell identities. *Mol Cell*, **38**, 576-589.

Helfer, A., Nusinow, D.A., Chow, B.Y., Gehrke, A.R., Bulyk, M.L. and Kay, S.A. (2011) LUX ARRHYTHMO encodes a nighttime repressor of circadian gene expression in the Arabidopsis core clock. *Curr Biol*, **21**, 126-133.

Herrero, E., Kolmos, E., Bujdoso, N., Yuan, Y., Wang, M., Berns, M.C., Uhlworm, H., Coupland, G., Saini, R., Jaskolski, M., Webb, A., Goncalves, J. and Davis, S.J. (2012) EARLY FLOWERING4 recruitment of EARLY FLOWERING3 in the nucleus sustains the Arabidopsis circadian clock. *Plant Cell*, **24**, 428-443.

Holm, M., Ma, L.G., Qu, L.J. and Deng, X.W. (2002) Two interacting bZIP proteins are direct targets of COP1-mediated control of light-dependent gene expression in Arabidopsis. *Genes Dev*, **16**, 1247-1259.

Hsu, P.Y. and Harmer, S.L. (2014) Wheels within wheels: the plant circadian system. *Trends Plant Sci*, **19**, 240-249.

Huang, W., Perez-Garcia, P., Pokhilko, A., Millar, A.J., Antoshechkin, I., Riechmann, J.L. and Mas, P. (2012) Mapping the core of the Arabidopsis circadian clock defines the network structure of the oscillator. *Science*, **336**, 75-79.

Huang, X., Ouyang, X. and Deng, X.W. (2014) Beyond repression of photomorphogenesis: role switching of COP/DET/FUS in light signaling. *Curr Opin Plant Biol*, **21**, 96-103.

Jing, Y., Zhang, D., Wang, X., Tang, W., Wang, W., Huai, J., Xu, G., Chen, D., Li, Y. and Lin, R. (2013) Arabidopsis chromatin remodeling factor PICKLE interacts with transcription factor HY5 to regulate hypocotyl cell elongation. *Plant Cell*, **25**, 242-256.

Kamioka, M., Takao, S., Suzuki, T., Taki, K., Higashiyama, T., Kinoshita, T. and Nakamichi, N. (2016) Direct Repression of Evening Genes by CIRCADIAN CLOCK-ASSOCIATED1 in the Arabidopsis Circadian Clock. *Plant Cell*, **28**, 696-711.

Kevei, E., Gyula, P., Feher, B., Toth, R., Viczian, A., Kircher, S., Rea, D., Dorjgotov, D., Schafer, E., Millar, A.J., Kozma-Bognar, L. and Nagy, F. (2007) Arabidopsis thaliana circadian clock is regulated by the small GTPase LIP1. *Curr Biol*, **17**, 1456-1464.

Kevei, E., Gyula, P., Hall, A., Kozma-Bognar, L., Kim, W.Y., Eriksson, M.E., Toth, R., Hanano, S., Feher, B., Southern, M.M., Bastow, R.M., Viczian, A., Hibberd, V.,

Davis, S.J., Somers, D.E., Nagy, F. and Millar, A.J. (2006) Forward genetic analysis of the circadian clock separates the multiple functions of ZEITLUPE. *Plant Physiol*, **140**, 933-945.

Lee, J., He, K., Stolc, V., Lee, H., Figueroa, P., Gao, Y., Tongprasit, W., Zhao, H., Lee, I. and Deng, X.W. (2007) Analysis of transcription factor HY5 genomic binding sites revealed its hierarchical role in light regulation of development. *Plant Cell*, **19**, 731-749.

Li, G., Siddiqui, H., Teng, Y., Lin, R., Wan, X.Y., Li, J., Lau, O.S., Ouyang, X., Dai, M., Wan, J., Devlin, P.F., Deng, X.W. and Wang, H. (2011) Coordinated transcriptional regulation underlying the circadian clock in Arabidopsis. *Nat Cell Biol*, **13**, 616-622.

Li, J., Li, G., Gao, S., Martinez, C., He, G., Zhou, Z., Huang, X., Lee, J.H., Zhang, H., Shen, Y., Wang, H. and Deng, X.W. (2010) Arabidopsis transcription factor ELONGATED HYPOCOTYL5 plays a role in the feedback regulation of phytochrome A signaling. *Plant Cell*, **22**, 3634-3649.

Lin, R., Ding, L., Casola, C., Ripoll, D.R., Feschotte, C. and Wang, H. (2007) Transposase-derived transcription factors regulate light signaling in Arabidopsis. *Science*, **318**, 1302-1305.

Lu, S.X., Webb, C.J., Knowles, S.M., Kim, S.H., Wang, Z. and Tobin, E.M. (2012) CCA1 and ELF3 Interact in the control of hypocotyl length and flowering time in Arabidopsis. *Plant Physiol*, **158**, 1079-1088.

Lu, X.D., Zhou, C.M., Xu, P.B., Luo, Q., Lian, H.L. and Yang, H.Q. (2015) Red-light-dependent interaction of phyB with SPA1 promotes COP1-SPA1 dissociation and photomorphogenic development in Arabidopsis. *Mol Plant*, **8**, 467-478.

Medzihradszky, M., Bindics, J., Adam, E., Viczian, A., Klement, E., Lorrain, S., Gyula, P., Merai, Z., Fankhauser, C., Medzihradszky, K.F., Kunkel, T., Schafer, E. and Nagy, F. (2013) Phosphorylation of phytochrome B inhibits light-induced signaling via accelerated dark reversion in Arabidopsis. *Plant Cell*, **25**, 535-544.

Mi, H., Huang, X., Muruganujan, A., Tang, H., Mills, C., Kang, D. and Thomas, P.D. (2017) PANTHER version 11: expanded annotation data from Gene Ontology and Reactome pathways, and data analysis tool enhancements. *Nucleic Acids Res*, **45**, D183-D189.

Mi, H., Muruganujan, A., Casagrande, J.T. and Thomas, P.D. (2013) Large-scale gene function analysis with the PANTHER classification system. *Nat Protoc*, **8**, 1551-1566.

Nakamichi, N., Kiba, T., Henriques, R., Mizuno, T., Chua, N.H. and Sakakibara, H. (2010) PSEUDO-RESPONSE REGULATORS 9, 7, and 5 are transcriptional repressors in the Arabidopsis circadian clock. *Plant Cell*, **22**, 594-605.

Nusinow, D.A., Helfer, A., Hamilton, E.E., King, J.J., Imaizumi, T., Schultz, T.F., Farre, E.M. and Kay, S.A. (2011) The ELF4-ELF3-LUX complex links the circadian clock to diurnal control of hypocotyl growth. *Nature*, **475**, 398-402.

Ouyang, Y., Andersson, C.R., Kondo, T., Golden, S.S. and Johnson, C.H. (1998) Resonating circadian clocks enhance fitness in cyanobacteria. *Proc Natl Acad Sci U S A*, **95**, 8660-8664.

Oyama, T., Shimura, Y. and Okada, K. (1997) The Arabidopsis HY5 gene encodes a bZIP protein that regulates stimulus-induced development of root and hypocotyl. *Genes Dev*, **11**, 2983-2995.

Palagyi, A., Terecskei, K., Adam, E., Kevei, E., Kircher, S., Merai, Z., Schafer, E., Nagy, F. and Kozma-Bognar, L. (2010) Functional analysis of amino-terminal domains of the photoreceptor phytochrome B. *Plant Physiol*, **153**, 1834-1845.

Pokhilko, A., Fernandez, A.P., Edwards, K.D., Southern, M.M., Halliday, K.J. and Millar, A.J. (2012) The clock gene circuit in Arabidopsis includes a repressilator with additional feedback loops. *Mol Syst Biol*, **8**, 574.

Rand, D.A. (2008) Mapping global sensitivity of cellular network dynamics: sensitivity heat maps and a global summation law. *J R Soc Interface*, **5 Suppl 1**, S59-69.

Schaffer, R., Ramsay, N., Samach, A., Corden, S., Putterill, J., Carre, I.A. and Coupland, G. (1998) The late elongated hypocotyl mutation of Arabidopsis disrupts circadian rhythms and the photoperiodic control of flowering. *Cell*, **93**, 1219-1229.

Sheerin, D.J., Menon, C., zur Oven-Krockhaus, S., Enderle, B., Zhu, L., Johnen, P., Schleifenbaum, F., Stierhof, Y.D., Huq, E. and Hiltbrunner, A. (2015) Light-activated phytochrome A and B interact with members of the SPA family to promote photomorphogenesis in Arabidopsis by reorganizing the COP1/SPA complex. *Plant Cell*, **27**, 189-201.

Southern, M.M., Brown, P.E. and Hall, A. (2006) Luciferases as reporter genes. *Methods Mol Biol*, **323**, 293-305.

Wang, Z.Y. and Tobin, E.M. (1998) Constitutive expression of the CIRCADIAN CLOCK ASSOCIATED 1 (CCA1) gene disrupts circadian rhythms and suppresses its own expression. *Cell*, **93**, 1207-1217.

Wenden, B., Kozma-Bognar, L., Edwards, K.D., Hall, A.J., Locke, J.C. and Millar, A.J. (2011) Light inputs shape the Arabidopsis circadian system. *Plant J*, **66**, 480-491.

Xu, D., Jiang, Y., Li, J., Lin, F., Holm, M. and Deng, X.W. (2016) BBX21, an Arabidopsis B-box protein, directly activates HY5 and is targeted by COP1 for 26S proteasome-mediated degradation. *Proc Natl Acad Sci U S A*, **113**, 7655-7660.

Yamamoto, Y., Sato, E., Shimizu, T., Nakamich, N., Sato, S., Kato, T., Tabata, S., Nagatani, A., Yamashino, T. and Mizuno, T. (2003) Comparative genetic studies on the APRR5 and APRR7 genes belonging to the APRR1/TOC1 quintet implicated in circadian rhythm, control of flowering time, and early photomorphogenesis. *Plant Cell Physiol*, **44**, 1119-1130.

FIGURE LEGENDS

Figure 1. Light-dependent short period phenotype of *hy5* and *hyh* mutants

(a) *CAB2:LUC* expression in WT (Ws), *hy5*, *hyh* and *hy5 hyh* plants. Seedlings were grown under 12 h white light / 12 h dark (12:12 LD) cycles for 7 days and transferred to continuous white light (WL) at 15 μmol m^{-2} s^{-1} fluence rate and luminescence was monitored.

(b) Free-running periods were estimated from *CAB2:LUC* rhythms in seedlings transferred to WL, continuous blue light (BL) or continuous red light (RL) at 15 μmol m^{-2} s^{-1} fluence rates. Error bars represent the standard error of data from 24 individual plants.

(c) Seedlings expressing *CCA1:LUC, GI:LUC or CCR2:LUC* were grown under 12:12 LD for 7 days and transferred to BL, RL or darkness (Dark). Luminescence rhythms were monitored for 6 days and free-running periods were estimated. Error bars represent the standard error of data from 24 individual plants. Asterisks indicate significant differences from the wild type as determined by Student's *t* test: * $P < 0.05$, ** $P < 0.01$, *** $P < 0.001$.

Figure 2. Light-dependent chromatin association of HY5

hy5 mutant plants carrying the *HY5:HY5-YFP* constructs were grown under 12:12 LD for 7 days, and harvested 52 h after transferred to BL or RL. Cross-linked and sonicated chromatin was immunoprecipitated with an α-GFP antibody. DNA was purified and subjected to NGS. HY5-bound promoters/genes were identified as described. Fold-enrichment was calculated by normalizing the peak heights to the corresponding counts from a mock (ChIP done without antibody) control.

(a) Venn-diagrams comparing gene list obtained in BL and RL.

(b) Venn-diagrams comparing the combined BL+RL gene list with the list of HY5-bound genes by Lee et al. 2007 and with list of clock and clock-associated genes (Hsu and Harmer, 2014).

(c) Fold-enrichment values of HY5 binding to genes present in both the BL and the RL samples were plotted, the colours of lines correspond to the actual light condition. Genes were sorted on the X axis by the increasing HY5 binding in RL.

(d) Fold-enrichment values of HY5 binding to clock and clock-associated genes (Hsu and Harmer, 2014) are plotted as bar graphs. Genes are not in particular order. Error bars represent standard error of three biological repeats.

Figure 3. Association of HY5 with promoters of clock genes is modulated by light quality

hy5 mutant plants carrying the *HY5:HY5-YFP* constructs were grown 12:12 LD for 7 days, transferred to BL or RL and harvested at ZT 48 and ZT 60. ZT 0 corresponds to the time of the transfer to BL or RL. Cross-linked and sonicated chromatin was immunoprecipitated with an α-GFP antibody. The mock sample was obtained from ChIP done on BL ZT 60 samples without antibody. DNA was purified and subjected to qPCR assays. Primers were designed to amplify 100-140 bp fragments lying within the identified ChIP-seq regions in *CCA1*, *PRR9*, *PRR5*, *LUX*, *ELF3*, *ELF4* and *GI* promoters. Intergenic refers to a control primer set specific to a genomic region between genes *At4g26900* and *At4g26910*. Enrichment was calculated by normalizing values to the signals measured in the initial non-immunoprecipitated (input) samples. Experiments were repeated 3 times **w**ith very similar results and a representative dataset is shown. Error bars represent the standard error of three technical repeats.

Figure 4. In vitro binding of HY5 to ACE elements present in the promoters of clock genes

(a) Sequence and position of ACE elements in the promoters of *CCA1*, *PRR9*, *PRR5*, *LUX*, *ELF3*, *ELF4* and *TOC1* genes. Positions are given relative to the transcription initiation site of

the corresponding gene, except for *PRR5* where positions are relative to the translation start site. The *cis*-elements are shown in capitals and the core ACE motif is highlighted by bold letters. Note that this is not a complete list of ACE-like elements present in the promoter of the above listed clock genes, but shows the ones that have been tested for in vitro binding HY5.
(b) Biotin-labelled double stranded probes (40 fmole) were incubated with expressed and purified HY5 proteins (400 ng). Binding reactions were resolved on 6 % native polyacrylamide gels. The 56-nuclotide long probes carried the wild-type or mutant derivatives of the indicated elements. Sequences of all probes are provided in Table S2. Bound (HY5-DNA complex) and non-bound (Free probe) probes are indicated. Asterisks mark non-specific bands, which appear independent of the presence of the HY5 protein. W: probe with wild-type ACE element, M: probe carrying the mutant derivative of the corresponding ACE element. Addition of HY5 protein to the binding reaction is indicated by - or + signs. Elements grouped by rectangles in panel **(a)** were located on a single probe fragment. Experiments were repeated 3 times with essentially the same results and a representative dataset is shown.

Figure 5. Temporal and light quality-dependent regulation of *HY5* and *HYH* expression
(a) to (b) WT (Ws) plants were grown under 12:12 LD for 7 days and transferred to BL or RL at 15 µmol m^{-2} s^{-1} fluence rates. Samples were harvested at the times indicated. *HY5* **(a)** and *HYH* **(b)** mRNA levels were determined by qPCR assays and normalized to the corresponding *TUBULIN* (*TUB*) mRNA levels. Error bars represent the standard error of 3 independent experiments.
(c) to (d) Plants carrying the *HY5:HY5-YFP* **(c)** or the *35S:HY5-YFP* **(d)** construct in the *hy5* mutant background were grown under 12:12 LD for 7 days and transferred to BL or RL or darkness (Dark). HY5-YFP fusion proteins were detected by Western-blots using an αGFP antibody. ACTIN was used as loading control. Experiments were repeated 4 times involving 2 independent transgenic lines for both constructs and representative datasets are shown.
(e) to (f) Plants carrying the *HYH:HYH-YFP* **(e)** or the *35S:HYH-YFP* **(f)** construct in the *hyh* mutant background were grown under 12:12 LD for 7 days and transferred to BL or RL. HYH-YFP fusion proteins were detected by Western-blots using an αGFP antibody. ACTIN was used as loading control. Experiments were repeated 3 times involving 2 independent transgenic lines for both constructs and representative datasets are shown.

Figure 6. Transcription of clock genes is affected by HY5 and HYH in a light quality-dependent manner

WT (Ws) and *hy5 hyh* mutant plants were grown under 12:12 LD for 7 days and transferred to BL or RL at 15 μmol m^{-2} s^{-1} fluence rates. Samples were harvested at the times indicated. *PRR5* **(a)**, *LUX* **(b),** *BOA* **(c)** and *CCA1* **(d)** mRNA levels were determined by qPCR assays and normalized to the corresponding *TUBULIN* (*TUB*) mRNA levels. Error bars represent the standard error of 3 independent experiments.

Figure 7. Modelling the clock in the *hy5 hyh* mutant.

De Caluwe model simulated mRNA expression of the four gene groups over one period cycle starting at peak of CL (CCA1/LHY) mRNA. **(a)** WT model with default parameters. Transcription rates are as follows: CL, v1=4.6; P97 (PRR7/PRR9) CL-independent rate, v2A=1.3 and CL-dependent rate v2B=1.5; P51 (PRR5/PRR1) rate, v3=1 and EL (ELF4/LUX) rate v4=1.5. Panel **(b)** shows the effect of increasing only P51 and EL rate parameters (v3 and v4) by 50%. In **(c)-(e)** additional effects of P97 transcription parameter changes are shown. Aside from increase of P51 and EL transcription parameters (v3 and v4, resp.) by 50%, in **(c)** and in **(d),** P97 CL-independent and CL-dependent rate parameters are each doubled, respectively. In **(e)** a change to same parameters is made as in **(d)**, but the changes are larger: P51 and EL rate parameters are doubled and P97 CL-dependent rate parameter (v2b) is increased to 4 (i.e. approx. 166.67%). In **(f)-(h)** effects of additional CL transcription parameter changes are shown. Aside from an increase of P51 and EL rate parameters by 50%, in **(f)** CL transcription rate constant (v1) is halved and in **(g)** CL transcription rate constant (v1) is decreased from 4.6 to 4.2, while P97 CL-dependent rate parameter (v2B) is doubled. In **(h)** P51 and EL rate parameters are doubled, while CL transcription parameter (v1) is decreased from 4.6 to 4.2 and P97 CL-dependent rate parameter (v2B) is increased to 4 (i.e., approx. 166.67%). Periods of the models are: **(b)** 24.57h, **(c)** 23.09h, **(d)** 22.78h, **(e)** 22.69h, **(f)** 22.99h, **(g)** 22.56h, **(h)** 22.47h.

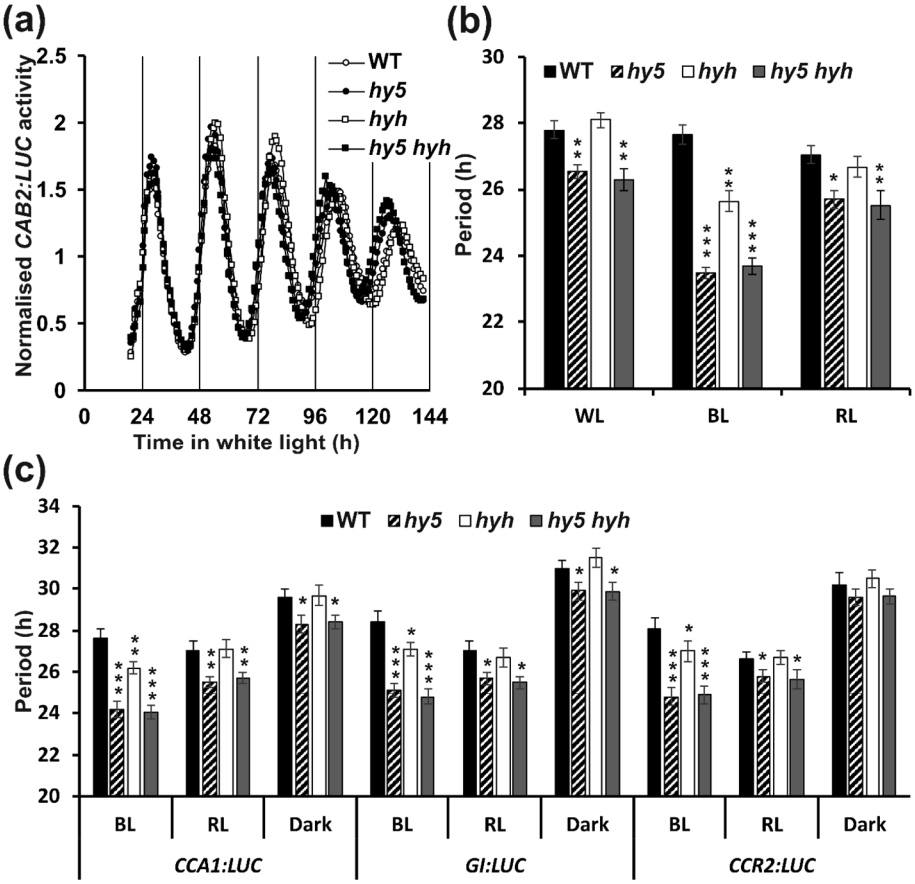

Figure 1. Light-dependent short period phenotype of *hy5* and *hyh* mutants
(a) *CAB2:LUC* expression in WT (Ws), *hy5*, *hyh* and *hy5 hyh* plants. Seedlings were grown under 12 h white light / 12 h dark (12:12 LD) cycles for 7 days and transferred to continuous white light (WL) at 15 µmol m^{-2} s^{-1} fluence rate and luminescence was monitored.
(b) Free-running periods were estimated from *CAB2:LUC* rhythms in seedlings transferred to WL, continuous blue light (BL) or continuous red light (RL) at 15 µmol m^{-2} s^{-1} fluence rates. Error bars represent the standard error of data from 24 individual plants.
(c) Seedlings expressing *CCA1:LUC, GI:LUC or CCR2:LUC* were grown under 12:12 LD for 7 days and transferred to BL, RL or darkness (Dark). Luminescence rhythms were monitored for 6 days and free-running periods were estimated. Error bars represent the standard error of data from 24 individual plants. Asterisks indicate significant differences from the wild type as determined by Student's *t* test: * $P < 0.05$, ** $P < 0.01$, *** $P < 0.001$.

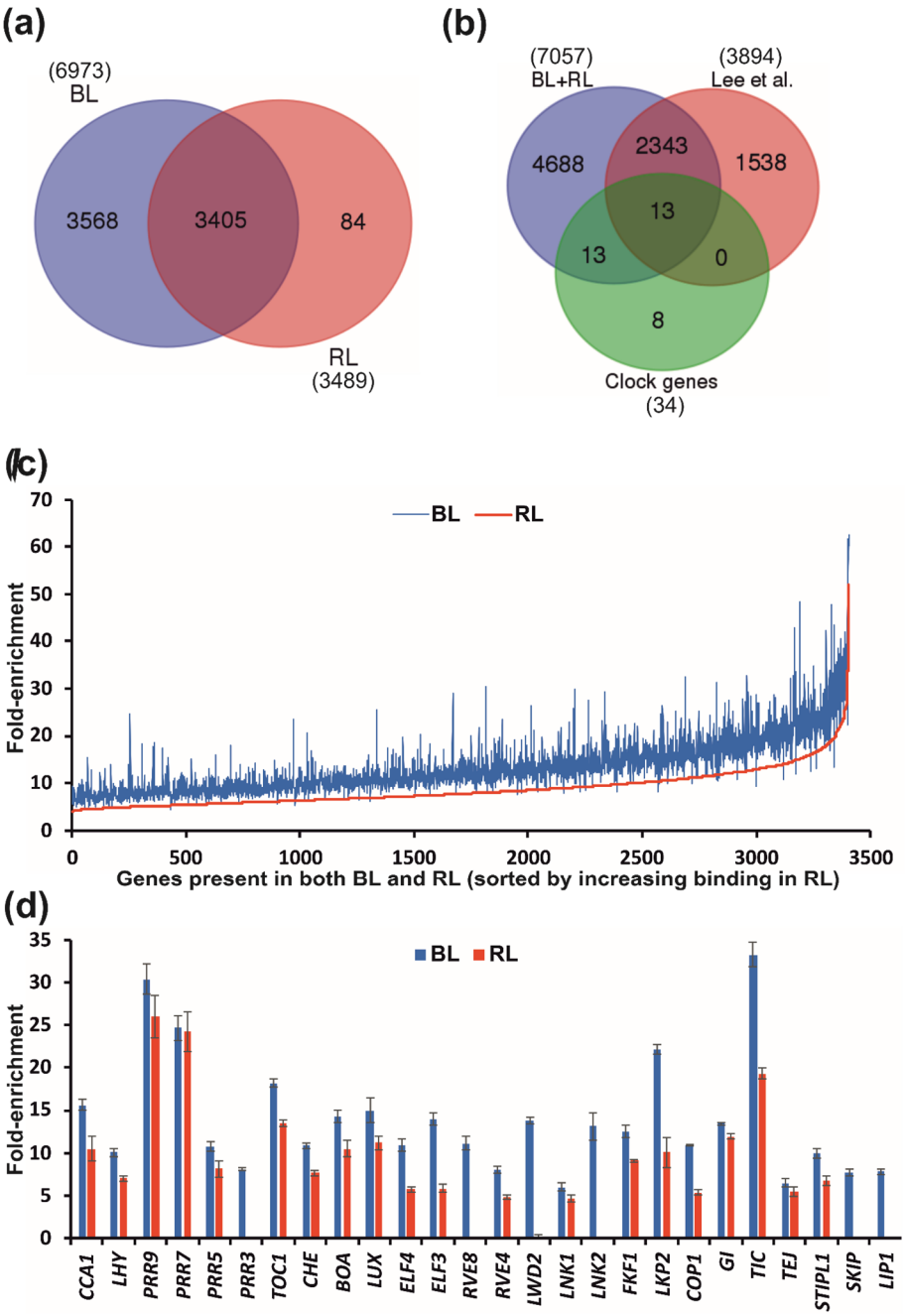

Figure 2. Light-dependent chromatin association of HY5
hy5 mutant plants carrying the *HY5:HY5-YFP* constructs were grown under 12:12 LD for 7 days, and harvested 52 h after transferred to BL or RL. Cross-linked and sonicated chromatin was immunoprecipitated with an α-GFP antibody. DNA was purified and subjected to NGS. HY5-bound promoters/genes were identified as described. Fold-enrichment was calculated by normalizing the peak heights to the corresponding counts from a mock (ChIP done without antibody) control.
(a) Venn-diagrams comparing gene list obtained in BL and RL.
(b) Venn-diagrams comparing the combined BL+RL gene list with the list of HY5-bound genes by Lee et al. 2007 and with list of clock and clock-associated genes (Hsu and Harmer, 2014).
(c) Fold-enrichment values of HY5 binding to genes present in both the BL and the RL samples were plotted, the colours of lines correspond to the actual light condition. Genes were sorted on the X axis by the increasing HY5 binding in RL.
(d) Fold-enrichment values of HY5 binding to clock and clock-associated genes (Hsu and Harmer, 2014) are plotted as bar graphs. Genes are not in particular order. Error bars represent standard error of three biological repeats.

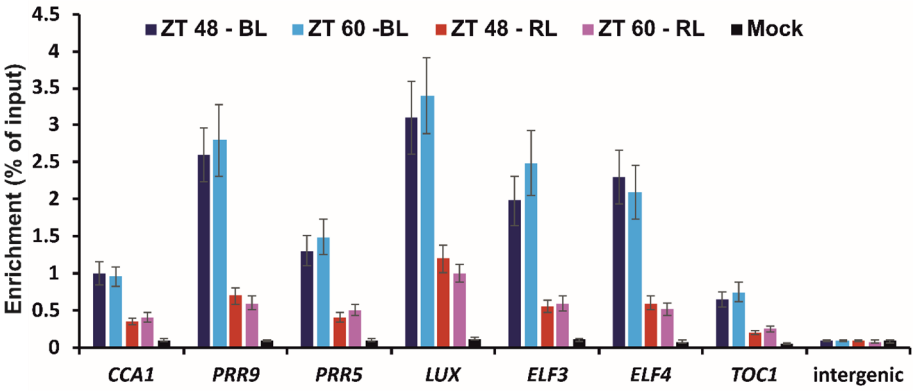

Figure 3. Association of HY5 with promoters of clock genes is modulated by light quality
hy5 mutant plants carrying the *HY5:HY5-YFP* constructs were grown 12:12 LD for 7 days, transferred to BL or RL and harvested at ZT 48 and ZT 60. ZT 0 corresponds to the time of the transfer to BL or RL. Cross-linked and sonicated chromatin was immunoprecipitated with an α-GFP antibody. The mock sample was obtained from ChIP done on BL ZT 60 samples without antibody. DNA was purified and subjected to qPCR assays. Primers were designed to amplify 100-140 bp fragments lying within the identified ChIP-seq regions in *CCA1*, *PRR9*, *PRR5*, *LUX*, *ELF3*, *ELF4* and *GI* promoters. Intergenic refers to a control primer set specific to a genomic region between genes *At4g26900* and *At4g26910*. Enrichment was calculated by normalizing values to the signals measured in the initial non-immunoprecipitated (input) samples. Experiments were repeated 3 times with very similar results and a representative dataset is shown. Error bars represent the standard error of three technical repeats.

(a)

cis-element	wild-type sequence	mutant derivatives
CCA1 G-box	-276 gaC**ACGT**Gtc -267	gaA**CATG**Ttc
PRR9 G/C-box	-125 gcC**ACGT**Cag -116	gcA**CATG**Aag
PRR5 T/G-box	*-321 caA**ACGT**Ggc -312	caC**CATG**Tgc
PRR5 G/C-box	*-313 gcC**ACGT**Cag -304	gcA**CATG**Aag
LUX G-box	-223 tcC**ACGT**Ggc -214	tcA**CATG**Tgc
LUX Z-box	-208 ctT**ACGT**Gcc -199	ctG**CATG**Tcc
ELF3 G/C-box	-87 tcC**ACGT**Cgt -78	tcA**CATG**Agt
ELF3 ACE	-178 ttt**ACGT**atc -169	ttt**CATG**atc
ELF4 A/C-box	-165 gaT**ACGT**Cta -156	gaG**CATG**Agc
ELF4 Z-box	-159 tcT**ACGT**Gag -150	gaG**CATG**Tag
TOC1 G/C-box	-161 tcC**ACGT**Cat -152	tcA**CATG**Aat

(b)

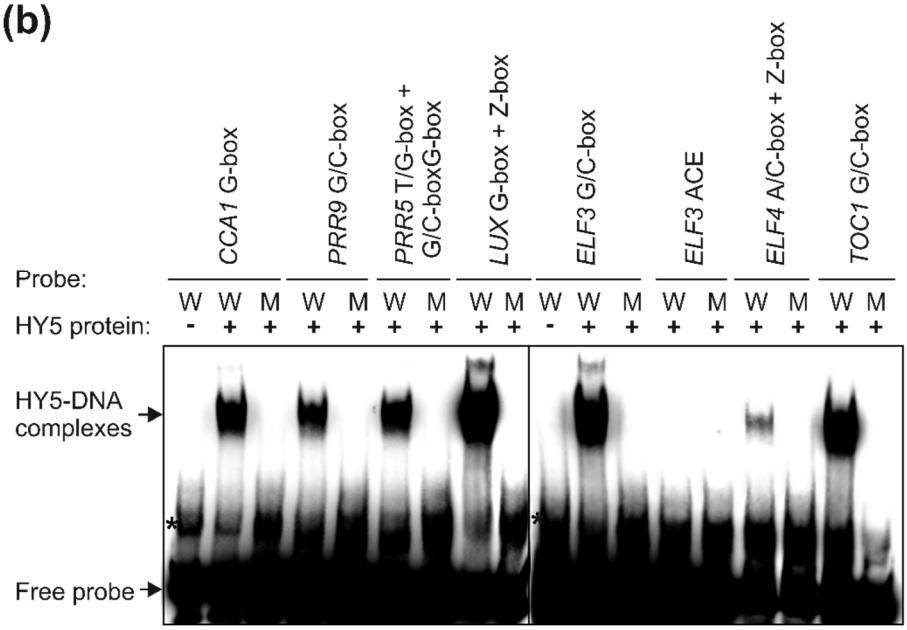

Figure 4. In vitro binding of HY5 to ACE elements present in the promoters of clock genes
(a) Sequence and position of ACE elements in the promoters of *CCA1*, *PRR9*, *PRR5*, *LUX*, *ELF3*, *ELF4* and *TOC1* genes. Positions are given relative to the transcription initiation site of the corresponding gene, except for *PRR5* where positions are relative to the translation start site. The *cis*-elements are shown in capitals and the core ACE motif is highlighted by bold letters. Note that this is not a complete list of ACE-like elements present in the promoter of the above listed clock genes, but shows the ones that have been tested for in vitro binding HY5.
(b) Biotin-labelled double stranded probes (40 fmole) were incubated with expressed and purified HY5 proteins (400 ng). Binding reactions were resolved on 6 % native polyacrylamide gels. The 56-nuclotide long probes carried the wild-type or mutant derivatives of the indicated elements. Sequences of all probes are provided in Table S2. Bound (HY5-DNA complex) and non-bound (Free probe) probes are indicated. Asterisks mark non-specific bands, which appear independent of the presence of the HY5 protein. W: probe with wild-type ACE element, M: probe carrying the mutant derivative of the corresponding ACE element. Addition of HY5 protein to the binding reaction is indicated by - or + signs. Elements grouped by rectangles in panel **(a)** were located on a single probe fragment. Experiments were repeated 3 times with essentially the same results and a representative dataset is shown.

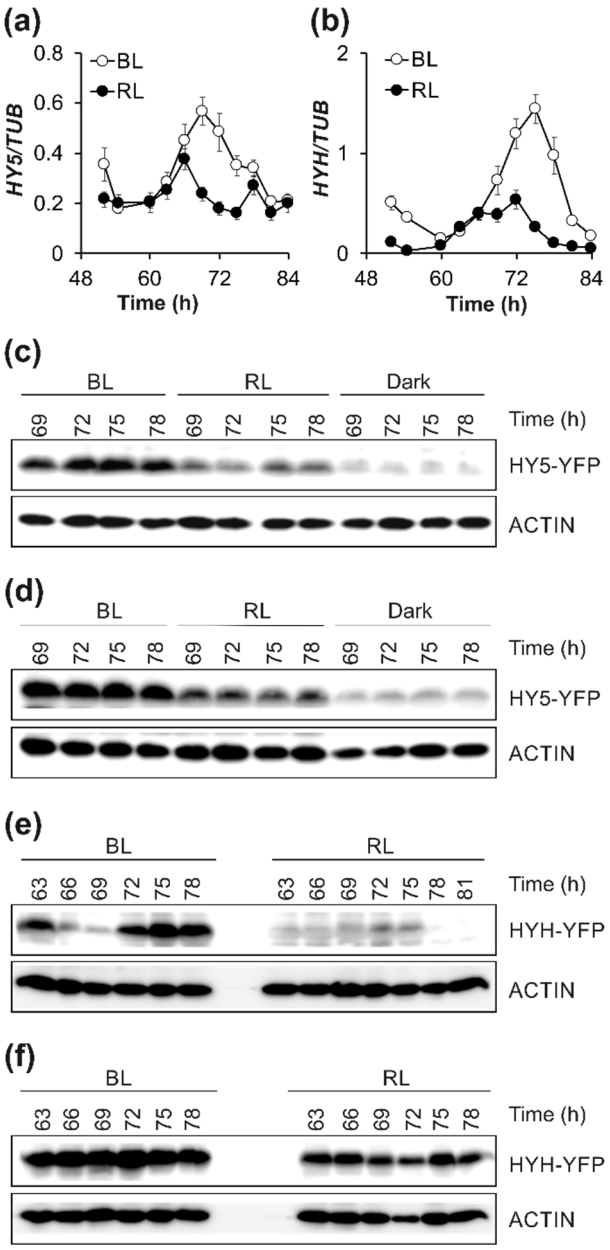

Figure 5. Temporal and light quality-dependent regulation of *HY5* and *HYH* expression
(a) to (b) WT (Ws) plants were grown under 12:12 LD for 7 days and transferred to BL or RL at 15 µmol m^{-2} s^{-1} fluence rates. Samples were harvested at the times indicated. *HY5* **(a)** and *HYH* **(b)** mRNA levels were determined by qPCR assays and normalized to the corresponding *TUBULIN* (*TUB*) mRNA levels. Error bars represent the standard error of 3 independent experiments.
(c) to (d) Plants carrying the *HY5:HY5-YFP* **(c)** or the *35S:HY5-YFP* **(d)** construct in the *hy5* mutant background were grown under 12:12 LD for 7 days and transferred to BL or RL or darkness (Dark). HY5-YFP fusion proteins were detected by Western-blots using an αGFP antibody. ACTIN was used as loading control. Experiments were repeated 4 times involving 2 independent transgenic lines for both constructs and representative datasets are shown.
(e) to (f) Plants carrying the *HYH:HYH-YFP* **(e)** or the *35S:HYH-YFP* **(f)** construct in the *hyh* mutant background were grown under 12:12 LD for 7 days and transferred to BL or RL. HYH-YFP fusion proteins were detected by Western-blots using an αGFP antibody. ACTIN was used as loading control. Experiments were repeated 3 times involving 2 independent transgenic lines for both constructs and representative datasets are shown.

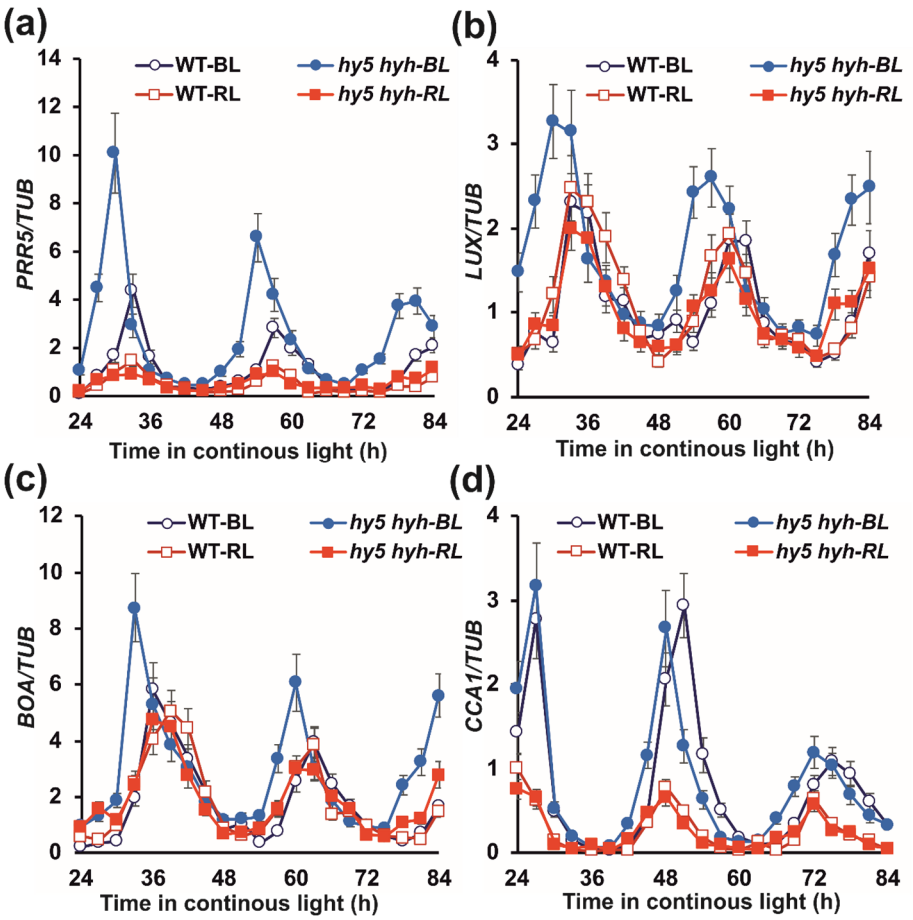

Figure 6. Transcription of clock genes is affected by HY5 and HYH in a light quality-dependent manner
WT (Ws) and *hy5 hyh* mutant plants were grown under 12:12 LD for 7 days and transferred to BL or RL at 15 µmol m^{-2} s^{-1} fluence rates. Samples were harvested at the times indicated. *PRR5* **(a)**, *LUX* **(b),** *BOA* **(c)** and *CCA1* **(d)** mRNA levels were determined by qPCR assays and normalized to the corresponding *TUBULIN* (*TUB*) mRNA levels. Error bars represent the standard error of 3 independent experiments.

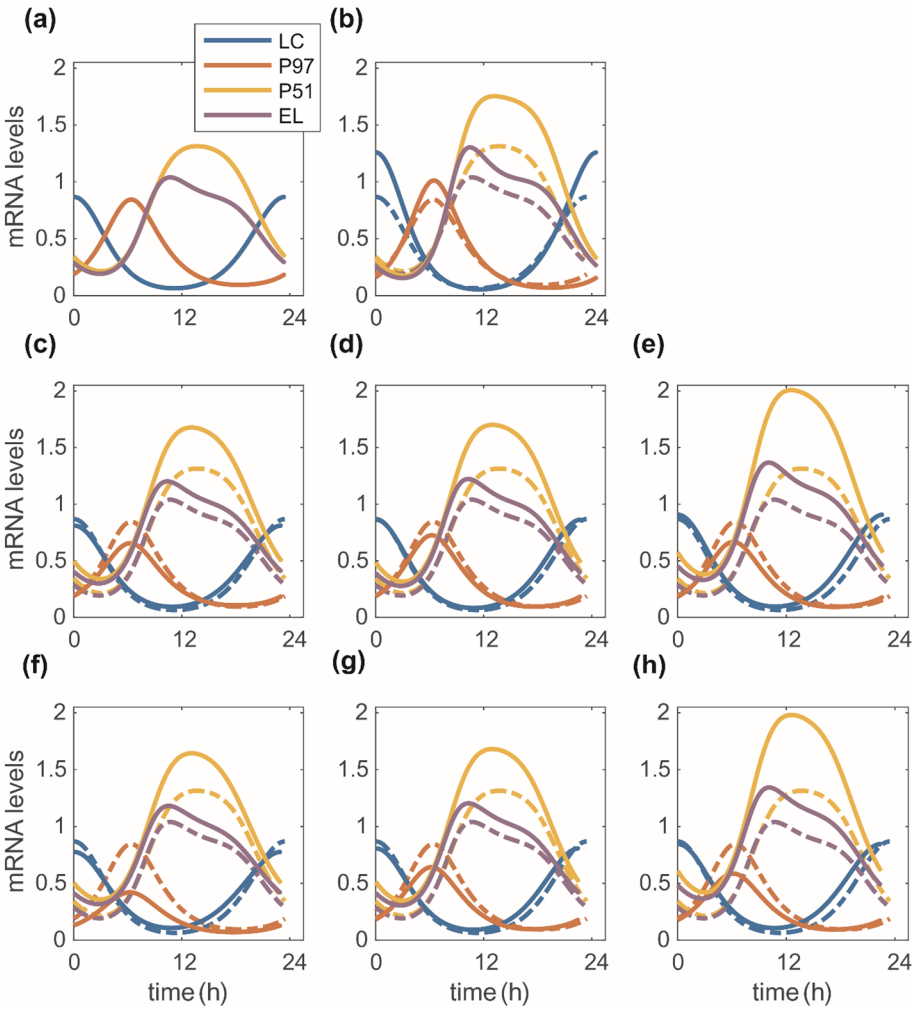

Figure 7. Modelling the clock in the *hy5 hyh* mutant.
De Caluwe model simulated mRNA expression of the four gene groups over one period cycle starting at peak of CL (CCA1/LHY) mRNA. **(a)** WT model with default parameters. Transcription rates are as follows: CL, v1=4.6; P97 (PRR7/PRR9) CL-independent rate, v2A=1.3 and CL-dependent rate v2B=1.5; P51 (PRR5/PRR1) rate, v3=1 and EL (ELF4/LUX) rate v4=1.5. Panel **(b)** shows the effect of increasing only P51 and EL rate parameters (v3 and v4) by 50%. In **(c)-(e)** additional effects of P97 transcription parameter changes are shown. Aside from increase of P51 and EL transcription parameters (v3 and v4, resp.) by 50%, in **(c)** and in **(d),** P97 CL-independent and CL-dependent rate parameters are each doubled, respectively. In **(e)** a change to same parameters is made as in **(d)**, but the changes are larger: P51 and EL rate parameters are doubled and P97 CL-dependent rate parameter (v2b) is increased to 4 (i.e. approx. 166.67%). In **(f)-(h)** effects of additional CL transcription parameter changes are shown. Aside from an increase of P51 and EL rate parameters by 50%, in **(f)** CL transcription rate constant (v1) is halved and in **(g)** CL transcription rate constant (v1) is decreased from 4.6 to 4.2, while P97 CL-dependent rate parameter (v2B) is doubled. In **(h)** P51 and EL rate parameters are doubled, while CL transcription parameter (v1) is decreased from 4.6 to 4.2 and P97 CL-dependent rate parameter (v2B) is increased to 4 (i.e., approx. 166.67%). Periods of the models are: **(b)** 24.57h, **(c)** 23.09h, **(d)** 22.78h, **(e)** 22.69h, **(f)** 22.99h, **(g)** 22.56h, **(h)** 22.47h.

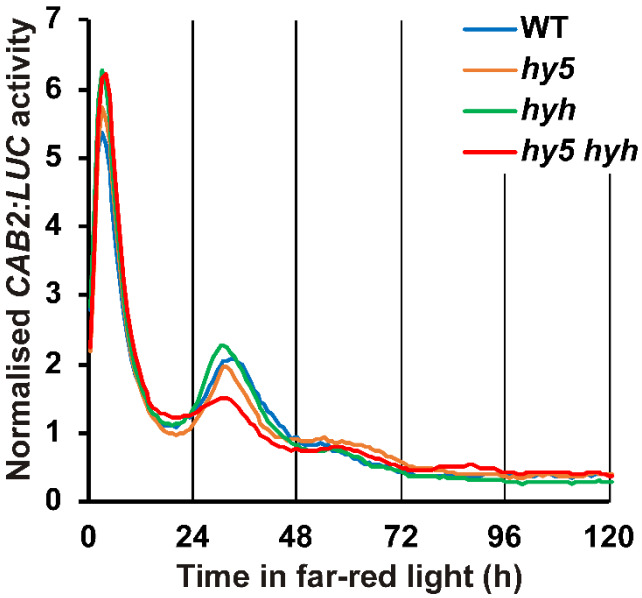

Figure S1. Low-amplitude rhythms of the *CAB2:LUC* reporter in continuous far-red light
CAB2:LUC expression was monitored in WT (Ws), *hy5*, *hyh* and *hy5 hyh* plants. Seedlings were grown under 12 h white light / 12 h dark (12:12 LD) cycles for 7 days and transferred to continuous far-red at 5 µmol m^{-2} s^{-1} fluence rate and luminescence was monitored.

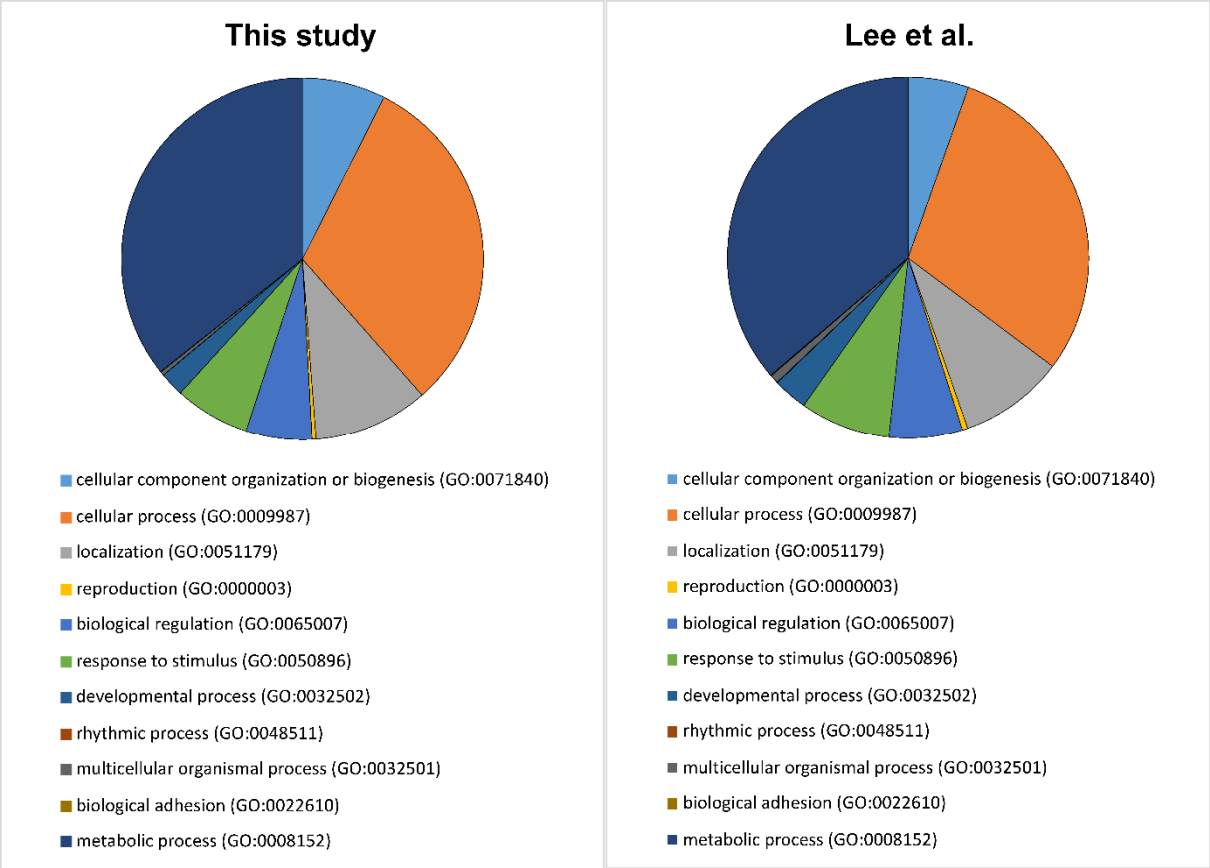

Figure S2. Distribution of functional (GO) categories within the HY5-bound genes identified by this study and by Lee *et al.*, 2007.

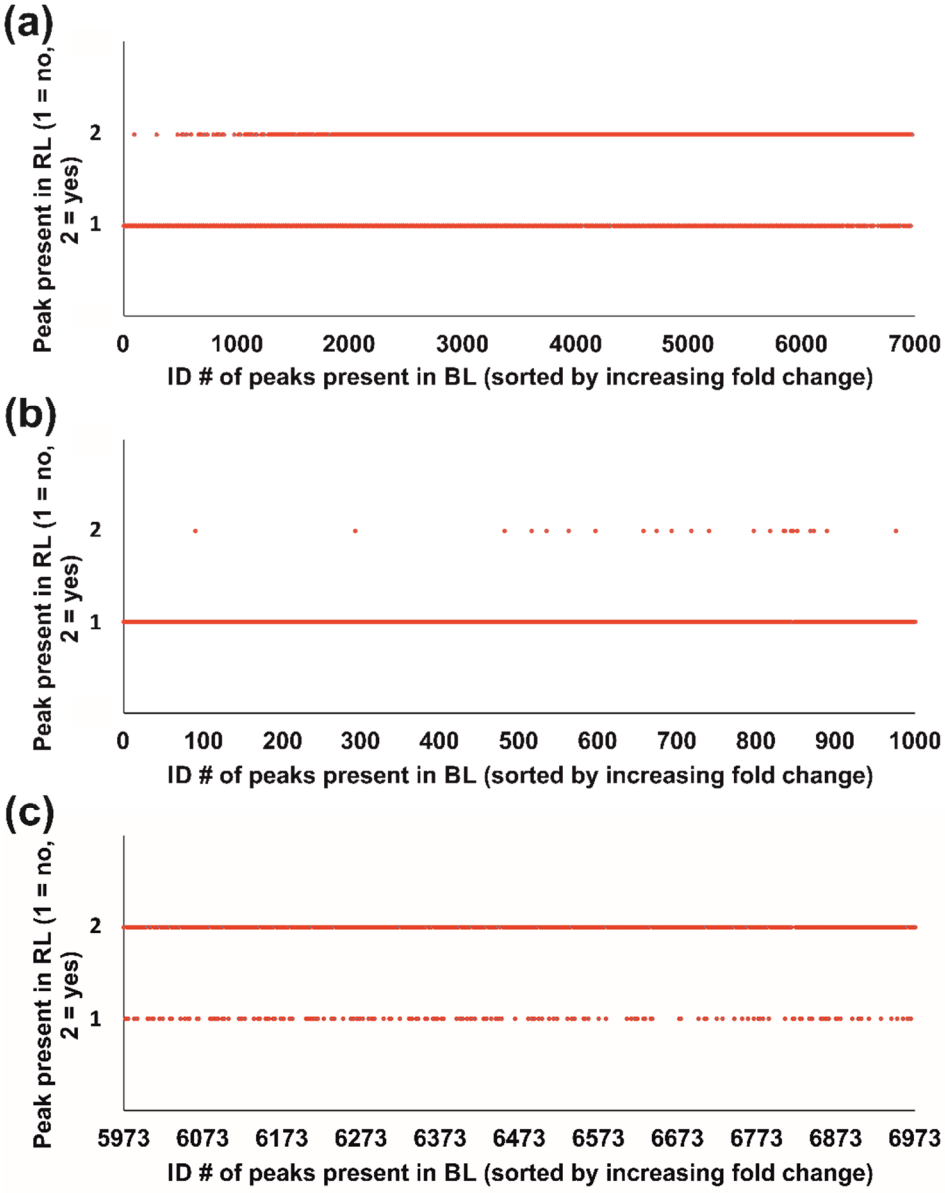

Figure S3. BL and RL gene lists are quantitatively different
All the genes that are bound by HY5 in BL were sorted along the X axis by their fold-enrichment values in BL. Values 2 or 1 on the Y axis were given if the particular gene was or was not found in the RL gene list, respectively. **(a)** shows the full range of genes, whereas **(b)** or **(c)** shows the first or the last 1000 genes, respectively.

Rank	Motif	P-value	log P-pvalue	% of Targets	% of Background	STD(Bg STD)	Best Match/Details	Motif File
1		1e-1158	-2.668e+03	48.26%	12.52%	40.9bp (92.0bp)	ABI5(bZIP)/col-ABI5-DAP-Seq(GSE60143) /Homer(0.997) More Information | Similar Motifs Found	motif file (matrix)
2		1e-345	-7.963e+02	25.12%	8.95%	55.1bp (81.2bp)	PCF/Arabidopsis-Promoters /Homer(0.920) More Information | Similar Motifs Found	motif file (matrix)
3		1e-184	-4.257e+02	32.15%	17.79%	45.0bp (85.4bp)	TGA10(bZIP)/colamp-TGA10-DAP-Seq(GSE60143) /Homer(0.830) More Information | Similar Motifs Found	motif file (matrix)
4		1e-171	-3.958e+02	44.07%	28.36%	55.2bp (73.3bp)	IDD2(C2H2)/colamp-IDD2-DAP-Seq(GSE60143) /Homer(0.781) More Information | Similar Motifs Found	motif file (matrix)
5		1e-104	-2.407e+02	47.23%	34.60%	63.9bp (82.0bp)	ATHB-15/MA1026.1 /Jaspar(0.819) More Information | Similar Motifs Found	motif file (matrix)

Figure S4. Top five de novo motif finding results from Homer
The full genome was used as background sequence.

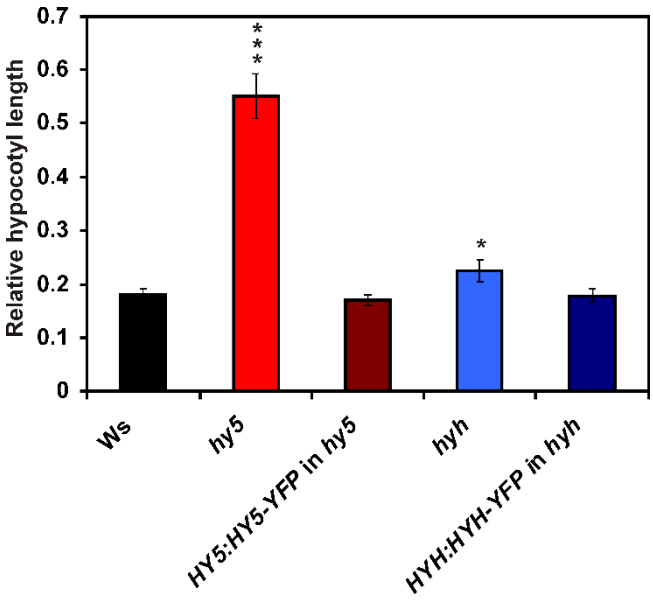

Figure S5. Complementation of the photomorphogenic phenotypes of *hy5* and *hyh* mutants by HY5-YFP and HYH-YFP proteins

WT (Ws), *hy5*, *hyh* seedlings and transgenic plants carrying the HY5:HY5-YFP construct in the *hy5* mutant background or the HYH:HYH-YFP construct in the *hyh* mutant background were grown in continuous blue light at 15 µmol m-2 s-1 fluence rate or in darkness for four days. Hypocotyl lengths were determined and normalized to the values from the corresponding dark-grown plants. Error bars represent the standard error of data from 30 to 40 individual plants. Asterisks indicate significant differences from the wild type as determined by Student's *t* test: * $P < 0.05$, *** $P < 0.001$.

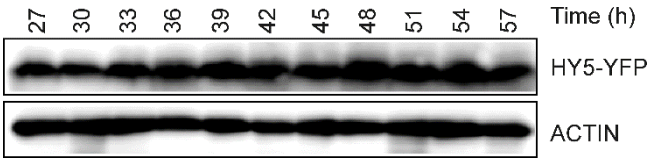

Figure S6. Non-rhythmic accumulation of the HY5-YFP fusion protein in continous blue light
Plants carrying the *HY5:HY5-YFP* construct in the *hy5* mutant background were grown under 12:12 LD for 7 days and transferred to BL. HY5-YFP fusion proteins were detected by Western-blots using an αGFP antibody. ACTIN was used as loading control. Experiments were repeated 3 times, a representative dataset is shown.


LHY mRNA
LHY/TUB
PRR9 mRNA
PRR9/TUB
PRR7 mRNA
PRR7/TUB
RVE8 mRNA
RVE8/TUB
RVE4 mRNA
RVE4/TUB
RVE6 mRNA
RVE6/TUB
PRR3 mRNA
PRR3/TUB
TOC1 mRNA
TOC1/TUB
CHE mRNA
CHE/TUB
ELF3 mRNA
ELF3/TUB
ELF4 mRNA
ELF4/TUB
ZTL mRNA
ZTL/TUB
Time in constant light (h)
WT-Blue
hy5 hyh-Blue

Figure S7. Clock or clock-associated genes showing unaltered mean expression levels in the *hy5 hyh* mutant versus WT in BL

WT (Ws) and *hy5 hyh* mutant plants were grown under 12:12 LD for 7 days and transferred to BL at 15 µmol m^{-2} s^{-1} fluence rates. Samples were harvested at the times indicated. mRNA levels of genes indicated were determined by qPCR assays and normalized to the corresponding *TUBULIN2/3* (*TUB*) mRNA levels. Error bars represent the standard error of 3 independent experiments.

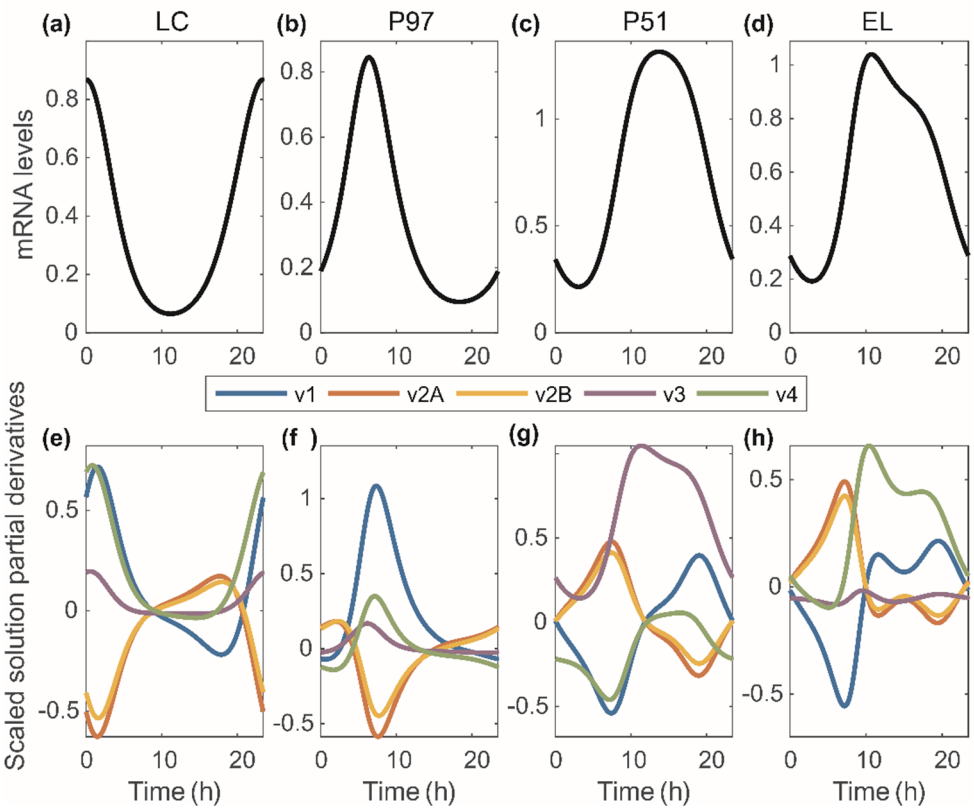

Figure S8. Simulated mRNA levels over one cycle and scaled solution derivatives.
(A-D) simulated default (WT) model mRNA levels over one cycle (period 23.4 h).
(E-H) Changes that will be made to mRNA levels as the parameters (listed) are changed.
Changes described are calculated as described in the theory from (Rand, 2008) and implemented in PeTTSy (Domijan *et al.,* 2016).

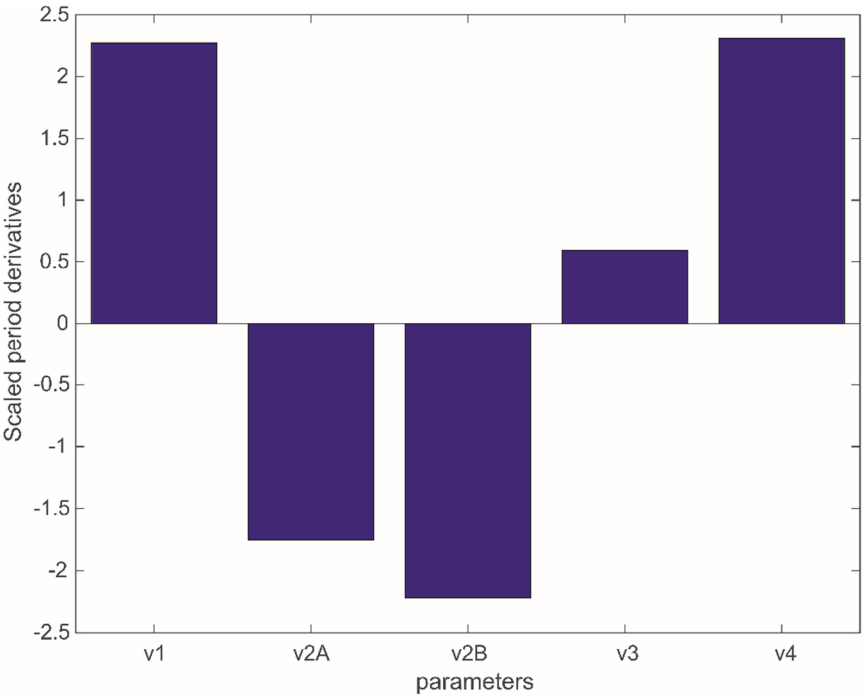

Figure S9. Barplot of the scaled period sensitivity coefficients of the model transcription rates. Transcription rates are: CL (v1); P97 CL-independent rate (v2A) and CL-dependent rate (v2B); P51 rate, (v3) and EL rate (v4). Calculations were performed using PeTTSy (Domijan *et al.*, 2016).

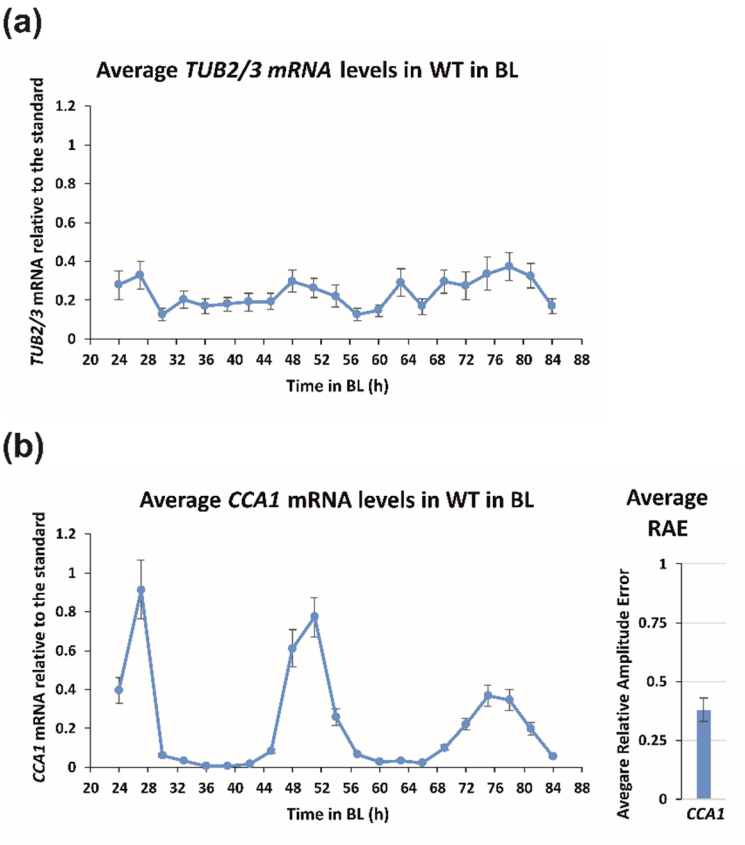

Figure S10. mRNA accumulation of TUBULIN 2/3 shows no circadian patterns under the conditions used in this work

WT (Ws) plants were grown under 12:12 LD for 7 days and transferred to BL at 15 µmol m^{-2} s^{-1} fluence rates. Samples were harvested at the times indicated and mRNA levels of genes indicated were determined by qPCR assays.

(a) *TUBULIN2/3* (*TUB2/3*) levels relative to the standard cDNA sample (see Experimental Procedures) are plotted. Average values of 3 independent experiments are shown. Error bars represent the standard error. Time series data from the 3 independent measurements were analysed by BRASS2, but no rhythmic traces with periods within the circadian interval (15-35 h) were detected.

(b) *CCA1* levels relative to the standard cDNA sample are plotted. Average values of 3 independent experiments are shown. Error bars represent the standard error. Time series data from the 3 independent measurements were analysed by BRASS2. All the 3 data series were rhythmic with average Relative Amplitude Error (RAE) of 0.38, indicating robust oscillations.

Dataset: genes present in both BL and RL (BL+RL)	**Table S1.**				
Analysis Type: PANTHER Overrepresentation Test (release 20170413)					
Annotation Version and Release Date:	GO Ontology database Released 2017-08-14				
Analyzed List:	BL+RL (Arabidopsis thaliana)				
Reference List:	Arabidopsis thaliana (all genes in database)				
Bonferroni correction:	TRUE				
Bonferroni count:	2166				
GO biological process complete	Arabidopsis thaliana - REFLIST (27060)	BL+RL (6911)	BL+RL (expected)	BL+RL (fold Enrichment)	BL+RL (P-value)
response to UV-B (GO:0010224)	**60**	**36**	**15.32**	**2.35**	**9.93E-03**
circadian rhythm (GO:0007623)	**85**	**47**	**21.71**	**2.17**	**3.57E-03**
rhythmic process (GO:0048511)	**102**	**56**	**26.05**	**2.15**	**4.88E-04**
protein dephosphorylation (GO:0006470)	80	43	20.43	2.1	1.87E-02
response to karrikin (GO:0080167)	103	55	26.31	2.09	1.43E-03
chloroplast organization (GO:0009658)	100	53	25.54	2.08	2.78E-03
plastid organization (GO:0009657)	136	69	34.73	1.99	3.84E-04
small molecule catabolic process (GO:0044282)	110	54	28.09	1.92	1.90E-02
response to cadmium ion (GO:0046686)	261	117	66.66	1.76	2.84E-05
response to water deprivation (GO:0009414)	232	101	59.25	1.7	9.68E-04
response to water (GO:0009415)	240	103	61.29	1.68	1.41E-03
vesicle-mediated transport (GO:0016192)	271	114	69.21	1.65	9.56E-04
response to osmotic stress (GO:0006970)	447	187	114.16	1.64	3.85E-07
response to salt stress (GO:0009651)	403	168	102.92	1.63	4.00E-06
intracellular protein transport (GO:0006886)	282	117	72.02	1.62	1.31E-03
response to metal ion (GO:0010038)	364	151	92.96	1.62	3.45E-05
cellular macromolecule localization (GO:0070727)	338	139	86.32	1.61	2.02E-04
response to inorganic substance (GO:0010035)	682	278	174.18	1.6	2.67E-10
cellular protein localization (GO:0034613)	314	126	80.19	1.57	2.58E-03
cofactor metabolic process (GO:0051186)	280	112	71.51	1.57	1.11E-02
response to alcohol (GO:0097305)	410	163	104.71	1.56	1.39E-04
response to abscisic acid (GO:0009737)	406	161	103.69	1.55	1.94E-04
protein transport (GO:0015031)	470	186	120.04	1.55	2.34E-05
intracellular transport (GO:0046907)	410	162	104.71	1.55	2.20E-04
establishment of protein localization (GO:0045184)	474	187	121.06	1.54	2.66E-05
response to cold (GO:0009409)	277	109	70.74	1.54	2.87E-02
small molecule biosynthetic process (GO:0044283)	479	188	122.33	1.54	3.47E-05
establishment of localization in cell (GO:0051649)	424	166	108.29	1.53	2.70E-04
protein localization (GO:0008104)	497	194	126.93	1.53	3.04E-05
response to abiotic stimulus (GO:0009628)	1492	578	381.05	1.52	4.55E-19
response to lipid (GO:0033993)	559	216	142.77	1.51	1.04E-05

response to light stimulus (GO:0009416)	563	217	143.79	1.51	1.16E-05
cellular localization (GO:0051641)	519	200	132.55	1.51	4.59E-05
response to temperature stimulus (GO:0009266)	405	156	103.44	1.51	1.57E-03
regulation of response to stimulus (GO:0048583)	403	154	102.92	1.5	2.84E-03
response to radiation (GO:0009314)	582	221	148.64	1.49	2.65E-05
response to bacterium (GO:0009617)	342	129	87.35	1.48	3.47E-02
peptide transport (GO:0015833)	528	195	134.85	1.45	1.14E-03
response to acid chemical (GO:0001101)	882	324	225.26	1.44	3.99E-07
response to oxygen-containing compound (GO:1901700)	1139	417	290.9	1.43	1.43E-09
amide transport (GO:0042886)	533	195	136.13	1.43	2.06E-03
organophosphate metabolic process (GO:0019637)	420	153	107.27	1.43	3.51E-02
organelle organization (GO:0006996)	863	312	220.41	1.42	4.19E-06
response to endogenous stimulus (GO:0009719)	1209	429	308.77	1.39	4.22E-08
response to hormone (GO:0009725)	1202	426	306.99	1.39	5.80E-08
response to organic substance (GO:0010033)	1466	510	374.41	1.36	9.12E-09
shoot system development (GO:0048367)	604	210	154.26	1.36	2.01E-02
response to chemical (GO:0042221)	2091	727	534.03	1.36	1.57E-13
carboxylic acid metabolic process (GO:0019752)	739	256	188.74	1.36	2.94E-03
cellular response to stress (GO:0033554)	586	202	149.66	1.35	4.79E-02
small molecule metabolic process (GO:0044281)	1193	410	304.69	1.35	5.16E-06
macromolecule localization (GO:0033036)	695	238	177.5	1.34	1.45E-02
nitrogen compound transport (GO:0071705)	674	229	172.14	1.33	3.48E-02
organic acid metabolic process (GO:0006082)	849	287	216.83	1.32	4.64E-03
oxoacid metabolic process (GO:0043436)	847	286	216.32	1.32	5.26E-03
post-embryonic development (GO:0009791)	1108	362	282.98	1.28	4.90E-03
cellular component organization (GO:0016043)	1658	539	423.45	1.27	2.95E-05
system development (GO:0048731)	1367	438	349.13	1.25	3.02E-03
transport (GO:0006810)	1738	556	443.88	1.25	1.32E-04
establishment of localization (GO:0051234)	1754	561	447.96	1.25	1.18E-04
localization (GO:0051179)	1817	579	464.05	1.25	1.14E-04
cellular response to stimulus (GO:0051716)	1976	627	504.66	1.24	5.47E-05
cellular biosynthetic process (GO:0044249)	3278	1038	837.19	1.24	8.80E-10
organic cyclic compound biosynthetic process (GO:1901362)	2019	639	515.64	1.24	5.66E-05
heterocycle biosynthetic process (GO:0018130)	1832	579	467.88	1.24	3.20E-04
aromatic compound biosynthetic process (GO:0019438)	1898	597	484.74	1.23	3.68E-04
organic substance biosynthetic process (GO:1901576)	3361	1057	858.38	1.23	2.53E-09
cellular component organization or biogenesis (GO:0071840)	1845	580	471.2	1.23	5.98E-04
signal transduction (GO:0007165)	1373	430	350.66	1.23	3.03E-02
developmental process (GO:0032502)	2332	729	595.58	1.22	3.52E-05

multicellular organism development (GO:0007275)	1961	613	500.83	1.22	5.45E-04
biosynthetic process (GO:0009058)	3580	1112	914.32	1.22	1.06E-08
organic cyclic compound metabolic process (GO:1901360)	3047	944	778.19	1.21	1.03E-06
cell communication (GO:0007154)	1553	481	396.63	1.21	2.73E-02
cellular aromatic compound metabolic process (GO:0006725)	2927	906	747.54	1.21	2.93E-06
heterocycle metabolic process (GO:0046483)	2818	871	719.7	1.21	8.32E-06
response to stimulus (GO:0050896)	4604	1421	1175.84	1.21	2.38E-11
anatomical structure development (GO:0048856)	2181	672	557.02	1.21	9.41E-04
regulation of gene expression (GO:0010468)	2182	668	557.27	1.2	2.31E-03
regulation of RNA metabolic process (GO:0051252)	1955	598	499.3	1.2	9.67E-03
regulation of transcription, DNA-templated (GO:0006355)	1931	590	493.17	1.2	1.27E-02
cellular macromolecule biosynthetic process (GO:0034645)	2233	682	570.3	1.2	2.38E-03
regulation of RNA biosynthetic process (GO:2001141)	1932	590	493.42	1.2	1.34E-02
regulation of nucleic acid-templated transcription (GO:1903506)	1932	590	493.42	1.2	1.34E-02
regulation of biosynthetic process (GO:0009889)	2120	647	541.44	1.19	5.02E-03
nucleobase-containing compound metabolic process (GO:0006139)	2581	787	659.18	1.19	4.08E-04
regulation of cellular biosynthetic process (GO:0031326)	2103	641	537.1	1.19	6.52E-03
regulation of nucleobase-containing compound metabolic process (GO:0019219)	1990	606	508.24	1.19	1.37E-02
cellular nitrogen compound metabolic process (GO:0034641)	3216	979	821.35	1.19	1.32E-05
cellular metabolic process (GO:0044237)	6383	1942	1630.19	1.19	5.77E-15
multicellular organismal process (GO:0032501)	2134	649	545.01	1.19	7.33E-03
macromolecule biosynthetic process (GO:0009059)	2273	691	580.51	1.19	3.62E-03
regulation of cellular macromolecule biosynthetic process (GO:2000112)	2056	625	525.09	1.19	1.18E-02
response to stress (GO:0006950)	2619	796	668.88	1.19	5.53E-04
regulation of macromolecule biosynthetic process (GO:0010556)	2057	625	525.35	1.19	1.25E-02
regulation of metabolic process (GO:0019222)	2433	739	621.38	1.19	1.71E-03
regulation of macromolecule metabolic process (GO:0060255)	2296	697	586.39	1.19	3.88E-03
regulation of nitrogen compound metabolic process (GO:0051171)	2186	662	558.29	1.19	9.61E-03
cellular nitrogen compound biosynthetic process (GO:0044271)	2289	693	584.6	1.19	5.83E-03
cellular macromolecule metabolic process (GO:0044260)	4370	1321	1116.08	1.18	6.95E-08
gene expression (GO:0010467)	2325	701	593.79	1.18	8.46E-03
regulation of primary metabolic process (GO:0080090)	2219	669	566.72	1.18	1.44E-02
regulation of cellular metabolic process (GO:0031323)	2282	687	582.81	1.18	1.27E-02
nitrogen compound metabolic process (GO:0006807)	5359	1613	1368.66	1.18	6.01E-10

nucleic acid metabolic process (GO:0090304)	2263	681	577.96	1.18	1.47E-02
regulation of cellular process (GO:0050794)	3544	1063	905.12	1.17	4.42E-05
regulation of biological process (GO:0050789)	3875	1161	989.66	1.17	1.02E-05
organonitrogen compound metabolic process (GO:1901564)	3312	986	845.87	1.17	5.71E-04
cellular process (GO:0009987)	8477	2522	2164.99	1.16	7.90E-17
primary metabolic process (GO:0044238)	6353	1872	1622.53	1.15	3.90E-09
organic substance metabolic process (GO:0071704)	6816	2007	1740.78	1.15	4.49E-10
biological regulation (GO:0065007)	4251	1251	1085.69	1.15	9.69E-05
macromolecule metabolic process (GO:0043170)	4830	1420	1233.56	1.15	1.04E-05
metabolic process (GO:0008152)	8032	2321	2051.34	1.13	2.66E-09
Unclassified (UNCLASSIFIED)	7962	2099	2033.46	1.03	0.00E+00
modification of morphology or physiology of other organism (GO:0035821)	280	33	71.51	0.46	5.58E-04
cell killing (GO:0001906)	253	22	64.62	0.34	1.47E-06
disruption of cells of other organism (GO:0044364)	253	22	64.62	0.34	1.47E-06
killing of cells of other organism (GO:0031640)	253	22	64.62	0.34	1.47E-06

Table S1. Gene Ontology Enrichment analysis of the combined BL+RL gene lists by PANTHER13 (Mi *et al*., 2017; Mi *et al*., 2013)

Table S2. Oligonucleotides for qPCR, ChIP qPCR and EMSA assays	
Primers for qPCR assays	
Primer ID	**Sequence (5' to 3')**
HY5 RT Fwd	CAGGCGACTGTCGGAGAAAGTCAAAGG
HY5 RT Rev	TCAACAACCTCTTCAGCCGCTTGTTCTC
HYH RT Fwd	ATTCTCTTCAACCTCTTACCTCTC
HYH RT Rev	AACTCCTCATCACTTTCCTCAG
PRR5 RT Fwd	GTGTATGTTGAAAGGTGCGG
PRR5 RT Rev	AGGAGCAAGTGAAGTTTGTC
LUX RT Fwd	GACGATGATTCTGATGATAAGG
LUX RT Rev	CAGTTTATGCACATCATATGGG
BOA RT Fwd	ACATATCCTTCTGTTGGTGGT
BOA RT Rev	CATAAGCCAAGAACCAGTATCTC
CCA1 RT Fwd	CTGTGTCTGACGAGGGTCGAA
CCA1 RT Rev	ATATGTAAAACTTTGCGGCAATACCT
LHY RT Fwd	CAACAGCAACAACAATGCAACTAC
LHY RT Rev	AGAGAGCCTGAAACGCTATACGA
PRR9 RT Fwd	GCCTTCTCAAGATTTGAGGAAAGC
PRR9 RT Rev	TTTGGCTCACCTGAAGTACTCTC
PRR7 RT Fwd	GTAGAAACTGTGATCTGGCCCTG
PRR7 RT Rev	GCACATTCCGATCATCCCTAA
RVE8 RT Fwd	GAAACCATATACCATCACCAAGTC
RVE8 RT Rev	TTCAATCTTCTTCCAGTCACGA
RVE4 RT Fwd	TATCTTCTTGACGACTTCTTGCTC
RVE4 RT Rev	ATGTTCCTCTTGTTTGTGACGA
RVE6 RT Fwd	CTGACTTTGAGGATCATAGACGG
RVE6 RT Rev	CAGGTGGGTCTTTGTTTAAGGT
PRR3 RT Fwd	AGGAATGAAAGTGGGAGTAGTG
PRR3 RT Rev	ATTGATTTGAAGGCGAGGTG
TOC1 RT Fwd	ATCTTCGCAGAATCCCTGTGATA
TOC1 RT Rev	GCACCTAGCTTCAAGCACTTTACA
CHE RT Fwd	GTTGACGGAAGAGGAAGAAGG
CHE RT Rev	TTGACCATCGGACTTGTGAC
ELF3 RT Fwd	CCATTGCCAATCAACAAAGAG
ELF3 RT Rev	CTGATCTCATCGAGCAAGAG
ELF4 RT Fwd	CGACAATCACCAATCGAGAATG
ELF4 RT Rev	AATGTTTCCGTTGAGTTCTTGAATC
ZTL RT Fwd	GGTATCGTGCTGAGGAAGTT
ZTL RT Rev	TCGGAAACAACCATAGAGTCA
GI RT Fwd	AATTCAGCACGCGCCTATTG
GI RT Rev	GTTGCTTCTGCTGCAGGAACTT
LKP2 RT Fwd	CTCTTGAACCTGACAACCCT
LKP2 RT Rev	AGAATCTACCATTGGATGCCT
FKF1 RT Fwd	AAGTCTTCACTGGCTATCGT
FKF1 RT Rev	TCTCAGATACAACCACAGGA
SKIP RT Fwd	TAGTAATATAGCAAGGCAATCGGG
SKIP RT Rev	ATCTACAGGCATCTCCACCA
LNK1 RT Fwd	CCTCAGACTCATCTCTTTCATCC
LNK1 RT Rev	TTCCTCTTGTTTCTCTATCCTCAG
LNK2 RT Fwd	TCTGTCATCCCAAAGTGTCC
LNK2 RT Rev	TTGTTGATATGGCTGGTCCT
JMJD5 RT Fwd	TACTCCGTTACACCATGATCC
JMJD5 RT Rev	AGAGCATTGTCTCAGAGTAAGG
LWD1 RT Fwd	GCATCCTTATCCACCAACGA
LWD1 RT Rev	ATCAGCGATTCTCCATAAACGA

LWD2 RT Fwd	CGATTATCTACGAGAGTGGTGAG
LWD2 RT Rev	TGCCCATGATAACAGTAGCC
TEJ RT Fwd	AGAAACTACTGCGTCACACC
TEJ RT Rev	ACACCATCATCTTCATGATCCT
TIC RT Fwd	CTCAAATCCTCAGACTCTTCCTC
TIC RT Rev	TCTCGGCTTCTTTCTCTTAGG
XCT RT Fwd	ATCTGGTCTTCTCCAATTCGG
XCT RT Rev	ATTAACCCTCTTCTCCACATACTC
COP1 RT Fwd	TCACAAGGAAATCACGAGAC
COP1 RT Rev	CTATCACTCTTCCAGCAAACC
TUB 2/3 RT Fwd	CCAGCTTTGGTGATTTGAAC
TUB 2/3 RT Rev	CAAGCTTTCGGAGGTCAGAG
Primers for ChIP qPCR assays	
Primer ID	**Sequence (5' to 3')**
CCA1 ChIP qPCR Fwd	GATTGTTGGTGAAGTAGTCGT
CCA1 ChIP qPCR Rev	CTTGATCTAGTGGGACCTACTTAA
PRR9 ChIP qPCR Fwd	GAATCAGCCGCGATACAGAG
PRR9 ChIP qPCR Rev	GACTTTGTTGTATAAGCTCAGAGC
PRR5 ChIP qPCR Fwd	GAAGGTTATTTGGCGTATTGGA
PRR5 ChIP qPCR Rev	CGGTTGTGGAAAGAGTATTTGG
LUX ChIP qPCR Fwd	CAAACACAACTTGCTAAGTCGG
LUX ChIP qPCR Rev	CAAACTAGGCACGTAAGATGGA
ELF3 ChIP qPCR Fwd	TTCTAGTTTCTTATTACAACGACA
ELF3 ChIP qPCR Rev	AAGATAGAAGGAGAGGATCTCT
ELF4 ChIP qPCR Fwd	TTCCTCTACCCAATCACTTCAC
ELF4 ChIP qPCR Rev	GAGTAAGTTCTGTTTCATCACCAC
TOC1 ChIP qPCR Fwd	CCAAACTATCCAACACAACCTT
TOC1 ChIP qPCR Rev	TGTAGCTTAATGGTGGGACTT
At4g26900/10 ChIP qPCR Fwd	TCTTATAGTTGATTTCCTTTTGTTGACAGT
At4g26900/10 ChIP qPCR Rev	GCTGAGAAAGTGAACATACGTTGCT
Oligonucleotides for EMSA assays	
Oligo ID	**Sequence (5' to 3')**
CCA1 W G-box EMSA Fwd BIOT	CCACTGATGTTTCTAGTGTATCAGA**CACGTG**TCGA CAAACTGGTGGGAGAGATTAA
CCA1 W G-box EMSA Rev	TTAATCTCTCCCACCAGTTTGTCGACACGTGTCTGA TACACTAGAAACATCAGTGG
PRR9 W G/C-box EMSA Fwd BIOT	ATCAAAACAATGGCTCATATTAAGC**CACGTC**AGCT CAGTGAAGGCCCGCTTTGTTA
PRR9 W G/C-box EMSA Rev	TAACAAAGCGGGCCTTCACTGAGCTGACGTGGCTT AATATGAGCCATTGTTTTGAT
PRR5 W T/G-box + G/C-box EMSA Fwd BIOT	CAGTATTTTGCTGATGTGGCA**AACGTG**GC**CACGTC** AGCCAATTCTACTAGATATTT
PRR5 W T/G-box + G/C-box EMSA Rev	AAATATCTAGTAGAATTGGCTGACGTGGCCACGTT TGCCACATCAGCAAAATACTG
LUX W G-box + Z-box EMSA Fwd BIOT	GACTTGGCTCTTTTCACTC**CACGTG**GCTCCATCT**TACGTG** CCTAGTTTGGTAATTT
LUX W G-box + Z-box EMSA Rev	AAATTACCAAACTAGGCACGTAAGATGGAGCCACGTGG AGTGAAAAGAGCCAAGTC
ELF3 W G/C-box EMSA Fwd BIOT	TCTTATTACAACGACAAAAAGAGTC**CACGTC**GTCACGCA CTTTTCCGGTGGTGAAA
ELF3 W G/C-box EMSA Rev	TTTCACCACCGGAAAAGTGCGTGACGACGTGGACTCTT TTTGTCGTTGTAATAAGA

ELF3 W ACE EMSA Fwd BIOT	ACATGGTAATATATCTATGACATTTT**ACGT**ATCCTAAAA GAAAACAAAAAGTGATG
ELF3 W ACE EMSA Rev	CATCACTTTTTGTTTTCTTTTAGGATACGTAAAATGTCAT AGATATATTACCATGT
ELF4 W A/C-box + Z-box EMSA Fwd BIOT	GTGTTCTTTGATATCAGATAGA**TACGTCTACGTG**AGATA CACGCTCTTGTTAATCA
ELF4 W A/C-box + Z-box EMSA Rev	TGATTAACAAGAGCGTGTATCTCACGTAGACGTATCTAT CTGATATCAAAGAACAC
TOC1 W G/C-box EMSA Fwd BIOT	TTTATGGCCTGCACTTTTTATTGTC**CACGTC**ATCTCCTTGG CCTAAAATATCCCAA
TOC1 W G/C-box EMSA Rev	TTGGGATATTTTAGGCCAAGGAGATGACGTGGACAATAA AAAGTGCAGGCCATAAA
CCA1 M G-box EMSA Fwd BIOT	CCACTGATGTTTCTAGTGTATCAGA**ACATGT**TCGACAAA CTGGTGGGAGAGATTAA
CCA1 M G-box EMSA Rev	TTAATCTCTCCCACCAGTTTGTCGAACATGTTCTGATACA CTAGAAACATCAGTGG
PRR9 M G/C-box EMSA Fwd BIOT	ATCAAAACAATGGCTCATATTAAGC**ACATGA**AGCTCAGT GAAGGCCCGCTTTGTTA
PRR9 M G/C-box EMSA Rev	TAACAAAGCGGGCCTTCACTGAGCTTCATGTGCTTAATA TGAGCCATTGTTTTGAT
PRR5 M T/G-box + G/C-box EMSA Fwd BIOT	CAGTATTTTGCTGATGTGGCA**CCATGT**GC**ACATGA** AGCCAATTCTACTAGATATTT
PRR5 M T/G-box + G/C-box EMSA Rev	AAATATCTAGTAGAATTGGCTTCATGTGCACATGG TGCCACATCAGCAAAATACTG
LUX M G-box + Z-box EMSA Fwd BIOT	GACTTGGCTCTTTTCACTC**ACATGT**GCTCCATCT**GCATGT** CCTAGTTTGGTAATTT
LUX M G-box + Z-box EMSA Rev	AAATTACCAAACTAGGACATGCAGATGGAGCACATGTG AGTGAAAAGAGCCAAGTC
ELF3 M G/C-box EMSA Fwd BIOT	ATCAAAACAATGGCTCATATTAAGC**ACATGA**AGCTCAGT GAAGGCCCGCTTTGTTA
ELF3 M G/C-box EMSA Rev	TAACAAAGCGGGCCTTCACTGAGCTTCATGTGCTTAATA TGAGCCATTGTTTTGAT
ELF3 M ACE EMSA Fwd BIOT	ACATGGTAATATATCTATGACATTTT**CATG**ATCCTAAAAG AAAACAAAAAGTGATG
ELF3 M ACE EMSA Rev	CATCACTTTTTGTTTTCTTTTAGGATCATGAAAATGTCAT AGATATATTACCATGT
ELF4 M A/C-box + Z-box EMSA Fwd BIOT	GTGTTCTTTGATATCAGATAGA**GCATGAGCATGT**AGATA CACGCTCTTGTTAATCA
ELF4 M A/C-box + Z-box EMSA Rev	TGATTAACAAGAGCGTGTATCTACATGCTCATGCTCTAT CTGATATCAAAGAACAC
TOC1 M G/C-box EMSA Fwd BIOT	TTTATGGCCTGCACTTTTTATTGTC**ACATGA**ATCTCCTTGG CCTAAAATATCCCAA
TOC1 M G/C-box EMSA Rev	TTGGGATATTTTAGGCCAAGGAGATTCATGTGACAATAAA AAGTGCAGGCCATAAA

Supplemental Table 2. Primers and oligonucleotides used in qPCR, ChIP qPCR and EMSA assays
W or M labels in the name of EMSA probes indicate that they carry the wild type (W) or the mutant derivates (M) of the corresponding cis-element. These elements are highlighted by bold letters in the sequence of the forward oligonucleotides. All the forward EMSA oligonucleotides were labeled by biotin (BIOT) at the 5' end.

SUPPORTING EXPERIMENTAL PROCEDURES

CHIP-SEQ ANALYSIS

Library preparation and sequencing Immunoprecipitated DNA samples were quantified using Qubit dsDNA HS Assay kit (Thermo Fischer Scientific). Library preparation was performed using NEBNext Ultra II DNA Library Prep Kit for Illumina (New England BioLabs) along with NEBNext Multiplex Oligos for Illumina (Index Primers Set 1 and 2, New England BioLabs) according to the manufacturer's protocol, except the following modifications: 1) since the amount of input DNA was less than 5ng, we used a 25-fold adaptor dilution for adaptor ligation; 2) adaptor-ligated DNA was cleaned up using AmPureXP Beads (Backman Coulter) without size selection; 3) PCR amplification was performed with 16 PCR cycles. Final libraries were quality checked using D1000 ScreenTape and Reagents on TapeStation 2200 (all from Agilent); quantification was performed using Qubit dsDNA BR Assay kit (Thermo Fischer Scientific). Sequencing was performed on Illumina MiSeq instrument using Illumina v2 500 cycle sequencing kit.

Bioinformatic Analysis

Quality control, trimming as well as read mapping were carried out in CLC Genomics Workbench Tool (CLC Bio, version: 9.5.4). Error probability of 0.05 (corresponding to Phred score 13) was used as a trimming quality threshold; up to 2 ambiguous nucleotides per read was allowed. Reads shorter than 36 nucleotides were removed. Reads were mapped onto *Arabidopsis thaliana* genome version TAIR10 with both the length and sequence identity parameters set to 0.8. Reads with multiple map positions (i.e. repeat reads) were randomly mapped.

Binary alignment files were exported to Homer (Heinz *et al.*, 2010) for downstream analysis. For each pulled sample as well as for the input, tag directories were generated with Homer command "makeTagDirectory". In addition, alignment files of biological replicates were merged and processed yielding pooled group tag directories. Homer script "findPeaks" was executed on each sample tag directory using ChIP-Seq analysis mode (-style factor) searching for enriched peaks as compared to the input. Peaks reported on the three separate biological replicates as well as on the pooled group alignment file were compared using Homer script "mergePeaks". For each biological group, peaks were filtered keeping only those ones that were detected in each separate replicate of the group as well as in the pooled "virtual" group sample. Peak annotation was carried out using a custom R script based on the Ensembl gene annotation with version TAIR10.34. Motif detection was carried out by Homer script

"findMotifsGenome.pl" on TAIR10 genome with fragment size set to 200 nucleotides and motif length set to 8 nucleotides.

Venn-diagrams were calculated using the on-line tool at http://bioinformatics.psb.ugent.be/webtools/Venn/. Functional categorization and GO term enrichment analysis of HY5-bound genes was done using PANTHER13 at http://www.pantherdb.org/ (Mi *et al.*, 2013, Mi *et al.*, 2017).

CIRCADIAN CLOCK MATHEMATICAL MODELS

Initially, three recent plant circadian clock models were considered for the analysis. These are the models from (Pokhilko *et al.*, 2012), (Fogelmark and Troein, 2014) and (De Caluwe *et al.*) and we will refer to them as Pokhilko 2012 and Fogelmark 2014 and de Caluwé models, respectively. The former two include a more detailed network structure with separate LUX, ELF3 and ELF4 components. Fogelmark 2014 additionally includes NOX clock component and models morning components LHY and CCA1 as repressors of PRRs, a feedback that was recently confirmed in (Adams *et al.*, 2015). De Caluwé model is a reduced model, based on the network of eight clock genes that have been grouped in four functional units: P51 (PRR5, TOC1), CL (CCA1, LHY), P97 (PRR7, PRR9) and EL (ELF4, LUX).

The first two models were discarded from further analysis, due to their inability to match the known *prr5* null mutant behavior. Both models were analysed in PeTTS toolbox (2016). Pokhilko 2012 model WT (default) period is 24.25h. The model includes an NI variable, which is a proxy for PRR5. Simulations of *prr5* null mutant were done by setting translation rate constant of NI to zero and this resulted in a model with oscillation period of 24.33h. Simulation of PRR5 overexpressor mutant was done by setting translation rate constant of NI to double of its WT value and this resulted in model oscillations with period of 24.45h. Since these simulations do not match the known information on the *PRR5* mutant period phenotypes (Eriksson *et al.*, 2003, Yamamoto *et al.*, 2003, Baudry *et al.*, 2010), the model was not considered for further analysis. Fogelmark 2014 model has 8 possible parameter value sets for the WT model. From these, only four sets (parameter sets identified as 1,2,6 and 7 from the paper) showed long-term sustained oscillations. Of these, only sets 1 and 2 had WT periods above 22.5h, and close to 24h, namely, 23.61h and 24.53h, respectively. Hence, only these two sets were considered for further analysis of the *prr5* null mutant behaviour. Model simulations were made by setting PRR5 translation rate set to 0 and 20% of its WT value, and in all cases, for both parameter sets, the simulations were arrhythmic in the long run. Since these simulations

do not match the known information on the *prr5* mutant period phenotypes, Fogelmark 2014 was also excluded from further analysis.

On the other hand, the de Caluwé model showed a short period phenotype when P51 translation was set low, with oscillation period of 23.12h if translation rate parameter of PRR51 was set to 50% of WT value, and period of 22.95h if the same rate constant was set to 0. The de Caluwé model showed an arrhythmic response when EL translation translate rate was set to zero, thus correctly matching the known *lux* mutant period behaviour (Hazen *et al.*, 2005). Based on this information, only de Caluwé model was be used for further analysis.

Sensitivity analysis

The model behaviour of interest are changes to model period, τ, and model solutions, g(t) that are functions of time t and represent time series of mRNA and protein levels.

Changes to model period, τ, brought on by changes to model parameters, k, can be explored using period partial derivatives, $\frac{\partial \tau}{\partial k}$. If an individual parameter k changes value from k_0 to k^*, then the change to the period can be approximated by $\frac{\partial \tau}{\partial k}(k_0) \cdot (k_0 - k^*) = \frac{\partial \tau}{\partial k}(k_0) \cdot \frac{(k_0 - k^*)}{k_0} \cdot k_0 = \frac{\partial \tau}{\partial \log(k)}(k_0) \cdot \frac{(k_0 - k^*)}{k_0}$

where the second fraction represents the relative change to the parameter value and the first term is the scaled period partial derivative. For a small enough relative change to several parameters, the change to period will be close to a weighted sum of the scaled period derivatives where the weights are the relative changes to the individual parameters. Figure S8 shows the scaled period derivatives of the de Caluwé model for all the transcription parameters of the model, as described in (Rand, 2008) and implemented in the toolbox PeTTSy (Domijan *et al.*, 2016).

Effect of the change to change in model solution, g(t) subject to change in parameter value k, can be approximated in a similar way, using partial derivative, $\frac{\partial g(t)}{\partial k}$. The change will be approximately, $\frac{\partial g(t)}{\partial \log(k)} \cdot \frac{(k_0 - k^*)}{k_0}$. Since the period can change with the change to parameters, one can calculate a scaled version of these partial derivatives, which do not change period but only indicate how the shape will change, as described in (Rand, 2008) and implemented in PeTTSy (Domijan *et al.*, 2016). These scaled partial solution derivatives for all transcription parameters of the model are given in (Fig. S9) showing the change to the model time series over one period

cycle subject to perturbation of each transcription parameter. An increase in transcription rate of P51, represented by parameter v_3, will lead to an overall increase in P51 mRNA simulated levels. Relative increase of 10% will approximately result in a change given by the scaled partial derivative (the one for v_3) multiplied by the factor of 0.1. This will result in an increase in P51 mRNA levels. On the other hand, the scaled partial derivative of EL mRNA solution for the same parameter is close to zero, so the same effect of this parameter on EL mRNA will be very small.

SUPPORTING REFERENCES

Adams, S., Manfield, I., Stockley, P. and Carre, I.A. (2015) Revised Morning Loops of the Arabidopsis Circadian Clock Based on Analyses of Direct Regulatory Interactions. *PLoS One*, **10**, e0143943.

Baudry, A., Ito, S., Song, Y.H., Strait, A.A., Kiba, T., Lu, S., Henriques, R., Pruneda-Paz, J.L., Chua, N.H., Tobin, E.M., Kay, S.A. and Imaizumi, T. (2010) F-box proteins FKF1 and LKP2 act in concert with ZEITLUPE to control Arabidopsis clock progression. *Plant Cell*, **22**, 606-622.

De Caluwe, J., Xiao, Q., Hermans, C., Verbruggen, N., Leloup, J.C. and Gonze, D. (2016) A Compact Model for the Complex Plant Circadian Clock. *Front Plant Sci*, **7**, 74.

Domijan, M., Brown, P.E., Shulgin, B.V. and Rand, D.A. (2016) PeTTSy: a computational tool for perturbation analysis of complex systems biology models. *BMC Bioinformatics*, **17**, 124.

Eriksson, M.E., Hanano, S., Southern, M.M., Hall, A. and Millar, A.J. (2003) Response regulator homologues have complementary, light-dependent functions in the Arabidopsis circadian clock. *Planta*, **218**, 159-162.

Fogelmark, K. and Troein, C. (2014) Rethinking transcriptional activation in the Arabidopsis circadian clock. *PLoS Comput Biol*, **10**, e1003705.

Hazen, S.P., Schultz, T.F., Pruneda-Paz, J.L., Borevitz, J.O., Ecker, J.R. and Kay, S.A. (2005) LUX ARRHYTHMO encodes a Myb domain protein essential for circadian rhythms. *Proc Natl Acad Sci U S A*, **102**, 10387-10392.

Heinz, S., Benner, C., Spann, N., Bertolino, E., Lin, Y.C., Laslo, P., Cheng, J.X., Murre, C., Singh, H. and Glass, C.K. (2010) Simple combinations of lineage-determining transcription factors prime cis-regulatory elements required for macrophage and B cell identities. *Mol Cell*, **38**, 576-589.

Mi, H., Huang, X., Muruganujan, A., Tang, H., Mills, C., Kang, D. and Thomas, P.D. (2017) PANTHER version 11: expanded annotation data from Gene Ontology and Reactome pathways, and data analysis tool enhancements. *Nucleic Acids Res*, **45**, D183-D189.

Mi, H., Muruganujan, A., Casagrande, J.T. and Thomas, P.D. (2013) Large-scale gene function analysis with the PANTHER classification system. *Nat Protoc*, **8**, 1551-1566.

Pokhilko, A., Fernandez, A.P., Edwards, K.D., Southern, M.M., Halliday, K.J. and Millar, A.J. (2012) The clock gene circuit in Arabidopsis includes a repressilator with additional feedback loops. *Mol Syst Biol*, **8**, 574.

Rand, D.A. (2008) Mapping global sensitivity of cellular network dynamics: sensitivity heat maps and a global summation law. *J R Soc Interface*, **5 Suppl 1**, S59-69.

Yamamoto, Y., Sato, E., Shimizu, T., Nakamich, N., Sato, S., Kato, T., Tabata, S., Nagatani, A., Yamashino, T. and Mizuno, T. (2003) Comparative genetic studies on the APRR5 and APRR7 genes belonging to the APRR1/TOC1 quintet implicated in circadian rhythm, control of flowering time, and early photomorphogenesis. *Plant Cell Physiol*, **44**, 1119-1130.